

# Acoustic-Seismic Detection of Ballistic-Missile Launches for Cooperative Early Warning of Nuclear Attack

Jürgen Altmann

---

Experimentelle Physik III, Universität Dortmund, Dortmund, Germany

In order to fill gaps in Russian early-warning systems, sensors can be deployed cooperatively near the silos of intercontinental ballistic missiles (ICBMs) that would sense a launch and would transmit continuously the information that no launch has occurred. The extremely loud launch noise propagates to kilometers and can be detected passively in all weather conditions by the induced ground motion. Buried seismic sensors minimize the intrusion and disturbance above the ground. Considerations of the propagation and acoustic-seismic transfer, as well as potential other sources of strong sound or ground motion, lead to the recommendation that acceleration sensors should be deployed at 0.1–1 km from each silo. Arrays of three sensors allow to estimate the azimuth and elevation of the source, improving discrimination from, e.g., overflying jet aircraft. The time course of signal amplitude, its maximum, and spectral characteristics provide additional characteristics to recognize a launch and other source types. One station would cost below \$50,000 so that all 800 ICBM silos of the USA and Russia can be covered at around \$40 million. Deployment can start after a development and testing phase of one to two years. Extension to mobile ICBMs and other nuclear states is possible.

## INTRODUCTION

### Improving Early Warning

Avoiding nuclear war from accidental or unauthorized use of nuclear weapons has been a concern already in the Cold War. Even though after

---

Received 24 February 2005; accepted 24 June 2005.

This research was funded by the Ploughshares Fund, San Francisco CA, USA. I would like to thank Frank von Hippel (Princeton University) and Steve Fetter (University of Maryland) for instigating this study and David Mosher (RAND Corporation) for providing literature.

Address correspondence to Jürgen Altmann, Experimentelle Physik III, Universität Dortmund, D-44221 Dortmund, Germany. E-mail: altmann@e3.physik.uni-dortmund.de

its end the likelihood of nuclear war growing out of a military confrontation, e.g., in Europe, has nearly vanished, the U.S. and Russia still have large numbers of weapons that are kept on high alert and require short decision times. Particularly problematic are the precise intercontinental ballistic missiles (ICBMs) in silos that can be targeted against each other.

In the 1990s, economic shortcomings led Russia to keep more of its mobile missiles in their garrisons and nuclear submarines at their bases, increasing their vulnerability to precise U.S. missiles that are being continuously improved. Furthermore, the Russian early warning system has deteriorated markedly: early warning satellites have not been replaced as needed, and a large formerly Soviet radar was lost because it was outside of Russia. Together with an existing gap in radar coverage, the result is that there are several hours every day during which Russia cannot convince itself that a missile attack is not underway.<sup>1</sup> In a potential future crisis, this would increase the nervousness; the same would hold at present, if there are erroneous indications of an attack without the ability to double-check. Several false alarms from the Cold War as well as after it illustrate what might happen in such an instance.<sup>2</sup>

One means of reducing the risk of inadvertent nuclear war is to increase the time for deciding about a possible counter-attack by reducing the alert status of nuclear missiles.<sup>3</sup> There have also been proposals to help Russia improve its early-warning system.<sup>4</sup>

A recent, thorough study from the US RAND Corporation has identified three types of scenarios of accidental or unauthorized use of a nuclear weapon: (a) unauthorized launch (by a rogue commander or terrorist), (b) launch by mistake (due to a training accident or a system malfunction), and (c) intentional launch based on incorrect information (due to a malfunction of the early-warning system, the incorrect interpretation of a nonthreatening event, the misperception of a nuclear attack by a third country or terrorists, the misperception of an accidental nuclear detonation on the own territory, or the misinterpretation of a simulated training attack as a real attack).<sup>5</sup> The study discussed 10 options of improving the situation under several criteria, and recommended “a phased approach for improving nuclear safety and U.S.-Russian relations.”

On the political level, U.S. and Russian presidents Clinton and Yeltsin at their 1998 summit meeting had already agreed to exchange information on missile launches and early warning, including setting up a possible center for exchange of missile-launch data, and expressed the intention to examine a multilateral prelaunch notification system with other states.<sup>6</sup> However, despite some preparations, a Joint Early Warning Center or a Joint Data Exchange Center has not yet been set up.

## Cooperative Monitoring of Ballistic-Missile Launches

Among the measures that the RAND study discussed and recommended for the near term is cooperative deployment of sensors at the silos of the ICBMs. The sensors would detect a launch and would provide a reliable confirmation as long as no missile has been launched.<sup>7</sup> The concept dates back at least to the 1980s, when R. L. Garwin proposed small radio units on the silo covers that would transmit as long as the covers remain closed.<sup>8</sup> In order to reduce the dangers of accidental and unauthorized nuclear launch, an international workshop in 1990 proposed several measures, among them “in-country early-warning systems operated by the other side.” An example would be (unspecified) sensors emplaced at the ICBM silos that “would continuously transmit coded signals as long as no missiles were launched and the sensors were not tampered with.”<sup>9</sup> If indications of an ICBM launch were seen by satellite or radar, but not by the silo sensors, that would be an indication of a false alarm. A proposal from the Russian Kurchatov Institute in 1999 mentioned several sensor types to be used for ICBMs in silos: optic loops, infrared sensors, smoke detectors, motion detectors, seismic sensors, radiation detectors, temperature sensors, and video cameras. Systems similar to those developed in U.S.-Russian cooperation for nuclear materials protection, control and accounting would monitor all strategic nuclear forces.<sup>10</sup> The RAND study of 2003 took these ideas up and discussed using seismic sensors outside ICBM silos, maybe including an optical-fiber seal across the silo door. Since silo-based ICBMs would remain central to a first strike—at least in the perception of both sides—the more intrusive extension to mobile ICBMs, sea-launched (submarine-based) ballistic missiles, and bombers, may not be needed. With several sensors per silo, the system could become robust against false alarms and could cost significantly less than other approaches for improving Russian early warning, in particular space-based ones.<sup>11</sup>

Beyond these general concepts, not much detail is available in the public literature. Sensors directly attached to the silos (e.g., signaling opening of the cover) would mean intrusion into a highly sensitive area. Of the sensor types that could be deployed at some distance, the optical ones (infrared sensors and video cameras) would be blocked by fog and heavy snowfall. Microphones would take up the strong launch noise, but would be exposed to the weather, requiring cleaning and maintenance. An additional disadvantage is that microphones could be spoofed relatively easily by loudspeakers at very close distance.<sup>12</sup> However, the launch noise also sets the ground into motion, and this motion can be sensed by seismic sensors that are completely closed and can be buried, minimizing the above-ground installation. Due to the large mass of soil involved, spoofing of seismic sensors would need much more energy and effort.

The present article is devoted to that concept. It analyzes the physics of seismic detection of ICBM launches and derives consequences for the design of the sensor system. The following section discusses the production of the launch

noise and the trajectory of the source. The next section describes the propagation to a position on the ground. How the arriving sound excites ground vibration that can be taken up by seismic sensors is the subject of the section after that. Aspects of detection and discrimination from other sources are treated in the next section. Then a section covers systems aspects including costs, and another presents conclusions and recommendations.

## BALLISTIC-MISSILE LAUNCH NOISE AND TRAJECTORY

### Propulsion and Noise Power

A ballistic missile is accelerated by the recoil of the hot exhaust gas emitted at high speed at the nozzle. A few characteristic parameters need to be introduced.<sup>13</sup> Most of the thrust force

$$F = \dot{m}v + (p_e - p_a)A_e, \quad (1)$$

is given by the mass flow rate  $\dot{m}$  times the exhaust velocity  $v$ ; if the pressure  $p_e$  at the exhaust is not equal to the ambient pressure  $p_a$ , the pressure difference times the nozzle exhaust area  $A_e$  adds another portion that increases as the missile climbs towards the vacuum of outer space. Often the second term is included by introduction of an effective exhaust velocity

$$v_e = F/\dot{m} = I_s g, \quad (2)$$

where  $g = 9.81$  m/s is the gravity acceleration at sea level and  $I_s$  the so-called specific impulse. The mechanical power of the exhaust gases is

$$P_{kin} = \dot{m}v^2/2 \approx Fv/2. \quad (3)$$

(In the second, approximate expression the pressure component of Eq. (1) has been neglected.) With temperatures above 2000 K and velocities above 2 km/s, the flow is supersonic and produces Mach waves in the surrounding air. Turbulent mixing is another source of noise. The mechanisms are complicated.<sup>14</sup> However, the acoustic efficiency,

$$\eta_{ac} = P_{ac}/P_{kin}, \quad (4)$$

the ratio of total radiated acoustic power  $P_{ac}$  to the mechanical power, is found to be close to 0.005 with an uncertainty around  $\pm 0.002$ .<sup>14,15</sup> Rockets and missiles produce extremely loud noise, much stronger than military aircraft with afterburner on. Table 1 shows important characteristics of U.S. and Russian intercontinental ballistic missiles; for acoustic-seismic monitoring, the first stage is the relevant one. Its burn time is typically 1 minute.

For the first stage of the U.S. Minuteman III (operational since 1970) very detailed information is available.<sup>16</sup> From the actual specific impulse  $I_s = 214$  s

**Table 1:** Characteristics of U.S. and Russian silo-based intercontinental ballistic missiles. (Sometimes, several values were given in the references.)

Type (Western designation)	Minuteman III <sup>a</sup>	Peacekeeper <sup>b</sup>	UR-100 NUTH (SS-19 Mod. 3) <sup>c</sup>	Topol-M (SS-27) <sup>d</sup>
Launch mass/kg	35,300; 34,500	87,500	105,600	47,200
Length/m	18.3	21.6	24.3 (with container)	22.7
Number of stages	3	4	2 + bus	3
Range/km	14,800; 12,900	10,700; > 13,000	10,000	> 10,000
Payload/kg	1,090; 680–910	3,580; 3,270	4,350	1,000
Number of warheads	2 or 3	10	6	1
Yield per wh./(kt TNT)	170 or 335–350	about 300	550–750	550
Fuel	Solid	Solid	Storable Liquid	Solid
First-stage diameter/m	1.67	2.33	2.5	1.86
Number of nozzles	4	1 <sup>e</sup>	4	—
First-stage thrust/MN	0.87	2.2	1.84	—
Remarks	—	Cold Launch <sup>f</sup>	—	Also Road-Mobile
		Originally Rail-Mobile		

<sup>a</sup>T. B. Cochran, W. M. Atkin, M. M. Hoening, *Nuclear Weapons Databook, Volume I—U.S. Nuclear Forces and Capabilities*, (Ballinger, Cambridge MA, 1984); Sutton (Note 13) pp. 263 f., 335.

<sup>b</sup>Cochran et al. (Note a); Peacekeeper (<http://www.astronautix.com/ls/peacper.htm>), (March 29, 2004).

<sup>c</sup>P. Podvig (ed.), *Russian Strategic Nuclear Forces*. (MIT Press, Cambridge MA/London, 2001).

<sup>d</sup>Podvig (Note c).

<sup>e</sup>McInerny 1996 (Note 15).

<sup>f</sup>Missile is ejected from canister by gas-generator pressure, engine ignites thereafter.

follows  $v_e = 2.10 \text{ km/s}$  after Eq. (1). The average thrust is  $F = 0.866 \text{ MN}$ , so from Eq. (2) the mass-flow rate  $\dot{m} = 412 \text{ kg/s}$ .<sup>17</sup> With Eq. (3), approximating  $v$  by  $v_e$ , the mechanical power of the gases is  $P_{kin} = 0.9 \text{ GW}$ , and from Eq. (4) with  $\eta_{ac} = 0.005$  follows an acoustic power  $P_{ac} = 4.5 \text{ MW}$ .

For a more modern solid-fuel missile such as the U.S. Peacekeeper (operational since 1986), a higher specific impulse can be assumed. With its first-stage thrust of 2.2 MN and a mass-flow rate  $\dot{m} = 802 \text{ kg/s}$ ,<sup>18</sup>  $v_e = 2.74 \text{ km/s}$  and  $I_{sp} = 280\text{s}$ .<sup>19</sup> With  $v$  slightly lower,  $P_{kin} \approx 3 \text{ GW}$ , and the acoustic power  $P_{ac} \approx 15 \text{ MW}$ .

For comparison: the thrust of large space-launch rockets is significantly higher—for the Saturn-V moon rocket (five LO<sub>2</sub>-Hydrocarbon-fueled booster engines with  $v_e = 2.6 \text{ km/s}$  at sea level), it was 33.7 MN, for the Space Shuttle (three LO<sub>2</sub>-LH<sub>2</sub>-fueled main engines with 3.6 km/s plus two solid-rocket boosters with 2.4 km/s) it is 29 MN.<sup>20</sup> Taking into account the partly higher exhaust velocities for the liquid-fuel engines, mechanical and thus acoustic powers are more than one order of magnitude above those of ICBMs.

## Typical Trajectory

Since the rocket mass decreases as burnt fuel leaves the nozzle, the acceleration increases during the burn time of each stage. For sensors at the ground, the first (and largest) stage is the relevant one. In order to reduce the drag from the lower layers of the atmosphere, ballistic missiles usually climb vertically for the first several kilometers. Typically, at burnout of the first stage an altitude of 25 km is reached at a speed of 1.5 km/s; depending on the trajectory chosen, the down-range distance can be 15–30 km. Figure 1 shows a computed trajectory during first-stage burn for a model missile without active trajectory control—the turn towards the optimum angle for maximum range is due to the action of gravity, starting with a fictitious deviation from vertical. Figure 2 shows the acceleration, velocity, altitude, and projected ground distance until burn-out of the fourth stage.

Since the acoustic amplitude decreases with distance from the source, sensors at the ground close to the launch location would sense the strongest signal during the beginning of the trajectory. Sensors farther away could experience a somewhat shorter distance to the source at a later time if the trajectory turns from the vertical and towards them in azimuth, but the minimum distance would nevertheless be tens of kilometers with the associated low amplitudes (see Figure 1).

From about 20 s after launch, the missile has supersonic speed, creating a Mach-wave cone. During the climb, this is directed upward and will not reach the ground. However, with sufficiently inclined trajectory the cone can touch the ground, giving rise to a strong sonic boom.<sup>21</sup> Since this effect and its location are very trajectory-dependent, it is not recommended as a reliable indication of a launch or no launch.

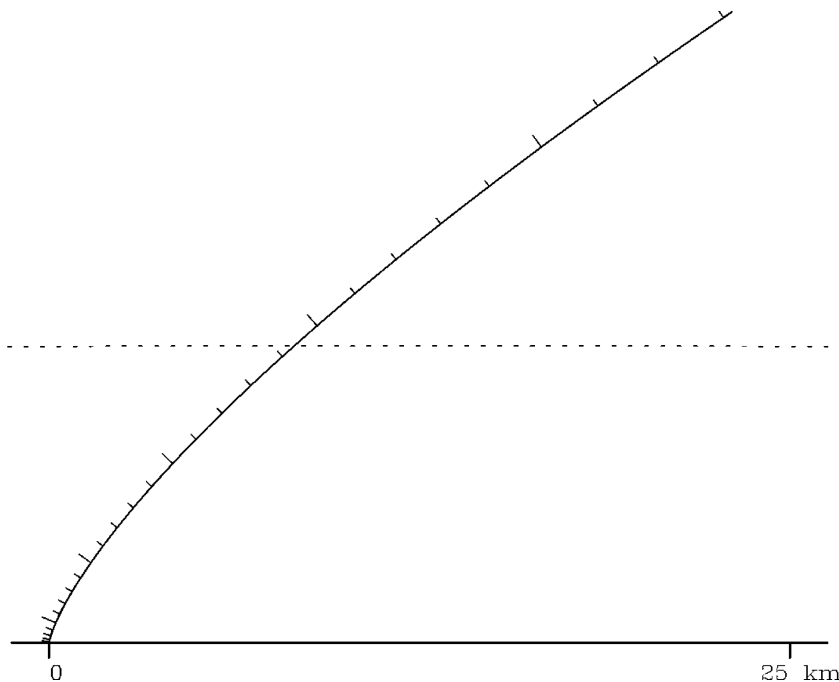


**Figure 1:** Launch trajectory to first-stage burnout for a model ballistic missile similar to the U.S. Peacekeeper, using gravity turn to achieve a maximum range of 10,800 km. The fourth-stage burnout occurs at 364 s in 509 km altitude, 1,528 km downrange, at angle 13.9° and speed 6.65 km/s.<sup>1</sup> One tick corresponds to 2 s. During first-stage burn, the acceleration increases from 13.5 to 44 m/s<sup>2</sup>; at the end, the speed is 1.4 km/s, the altitude 21 km and the down-range distance 23 km. The sound speed of 0.33 km/s is transcended at 20 s in 2.8 km altitude. Because in actual missiles the trajectory is controlled actively with vertical climb at first, deviations in burn-out altitude and down-range distance are probable. In the present model, the separated first stage reaches a maximum altitude of 50 km, hitting ground level 207 km from the launch point.

<sup>1</sup>Computed with the program KMRAk, described in J. Altmann, *SDI for Europe? Technical Aspects of Anti-Tactical Ballistic Missile Defenses*, PRIF Research Report 3/1988, Hessische Stiftung Friedens- und Konfliktforschung, Frankfurt/M. (1988). The program includes height-dependent gravity, air density, sound velocity, and Mach-number-dependent drag coefficient. Smaller effects such as earth rotation or lift during boost are neglected, the boost-phase trajectory is not controlled actively. Input data were mostly taken from Peacekeeper Specifications (Note 18) taking into account that the mass figures are rounded to 1000 or 100 pounds. I have not tracked the specifications to official sources, since 1. they seem plausible and 2. the exact details are not important here—thus, the rocket is denoted as the “model ballistic missile.” The first-stage exhaust area was derived from McLernon (note 15), the other areas and all exhaust pressures were estimated with rough nozzle sizes from a missile sketch, Peacekeeper Specifications (Note 18). Input data used: empty-stage masses 3,700, 2,700, 630, 545 kg; fuel masses 45,300, 24,500, 7,080, 635 kg; burn times 56.5, 60.7, 72.0, 168.0 s, exhaust velocities 2.52, 3.02, 2.93, 2.92 km/s; exhaust pressures 122, 15, 24, 22 kPa; exhaust areas 1.66, 3.46, 0.68, 0.17 m<sup>2</sup>, stage cross sections all 4.3 m<sup>2</sup>, stage delays all 2 s, low-speed drag coefficients all 0.25, payload 3,600 kg, re-entry vehicle: mass 200 kg, cross section 0.24 m, low-speed drag coefficient 0.15. The payload mass (given as 2,100 kg) was at first increased to 2,900 kg to have the sums add up to the total mass (given as 88,400 kg—Cochran et al. (Note a of Table 1) give 87,500 kg), then it was further increased to 3,600 kg where the maximum achievable range was about 10,800 km.

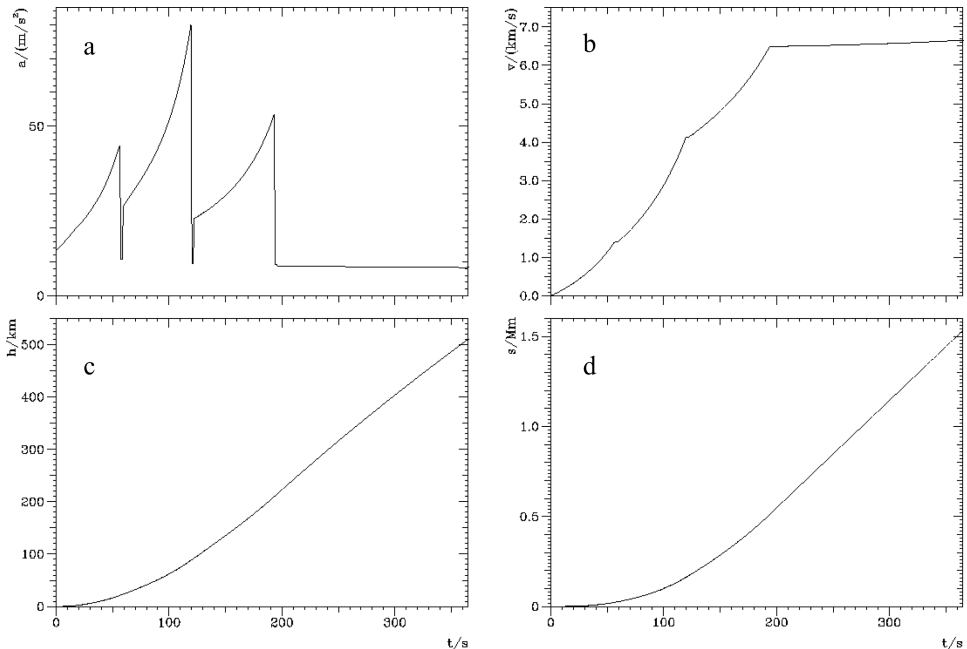


**Figure 2:** Kinematic quantities of the model ballistic missile of Figure 1 from launch to burnout of the final (here fourth) stage: (a) acceleration, (b) velocity, (c) altitude, (d) distance of ground-projection point from launch point.

Another Mach cone is produced when the first stage reenters the lower atmosphere—and here the shock waves are directed toward the ground always. Sonic booms from reentering first stages have indeed been observed directly or after coupling into the soil by seismic excitation—even thousands of kilometers away. At such large distances, only infrasound remains and multiple reflections are needed that depend on stratospheric wind conditions, and the amplitudes are very weak.<sup>22</sup> Even though the sonic boom should be detectable reliably in the reentry region, it is not optimal for launch detection for several reasons: The reentry location varies strongly with the trajectory chosen and can be more than 250 km distance from the launch site, thus a large area would have to be covered. Second, it arrives with a delay of more than four minutes after launch. Finally, a sonic boom is also produced by supersonic aircraft; differentiation from such events would require complex consideration of signals from many sensors.<sup>23</sup>

## Source Characterization

Acoustic emission from a burning missile engine is produced by two major effects.<sup>24</sup> At the margin of the supersonic jet flow there is turbulent mixing with the outside air. Vortices form, grow, coalesce, and disintegrate. With growing entrainment of air, the core of laminar flow gets thinner. At larger distances from the nozzle large irregular three-dimensional structures form. The

turbulent-mixing noise is broadband and highly directional, peaking around  $30^\circ$  from the exhaust axis. The second source comes from oblique shock waves and expansion fans that are first generated at the nozzle lip and are then reflected back into the jet at the jet boundary several times, forming so-called shock cells with a quasi-periodic pattern. As large-scale turbulence structures pass through the cells, interaction with the shock waves produces acoustic emission. Since various waveguide modes contribute, the combined emission creates a relatively small spectral peak. This so-called broadband shock-associated noise radiates mainly in directions forward of  $90^\circ$ . Under certain conditions, acoustic waves traveling backwards outside of the jet and influencing the nozzle lip, can form a feedback loop, intensifying one single frequency. Nonlinear steepening of wave fronts due to higher sound speed in higher pressure will then create harmonics, too. When this so-called screech tone occurs, it also radiates mainly in a forward direction.

Jet noise production is a field of active theoretical and experimental research. Empirical studies and models have used scaling laws to account for different rocket types.<sup>25</sup> The acoustically active plume has a length of about  $5 L_C$  with the maximum sound power emitted at about  $2 L_C$  where  $L_C$  is the length of the laminar core, approximated by  $L_C = (16-20) \cdot D_e$  (Figure 3).<sup>26</sup> The flow remains supersonic for a longer length, namely  $L_{SC} = (25-35) \cdot D_e$ .<sup>27</sup> The far-field directivity can be described using the Strouhal number

$$Sr = f D_e / v, \quad (5)$$

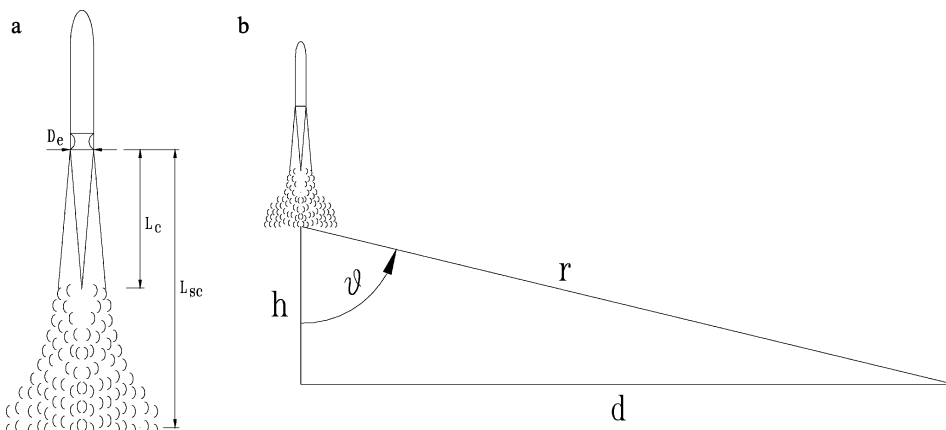


**Figure 3:** Turbulent mixing with the surrounding air of the gas jet leaving the exhaust of diameter  $D_e$  reduces the laminar-flow portion; beyond the length  $L_C$  of the laminar core, all flow is turbulent, staying supersonic to a greater length  $L_{SC}$  (a). The strength of the emitted sound varies with distance from the exhaust nozzle, frequency and angle  $\vartheta$  from the jet axis (b). The maximum emission occurs at about  $2 L_C$ ; the direction of strongest emission varies with frequency between  $\vartheta = 30^\circ$  for low frequencies and  $\vartheta = 60^\circ$  for high ones. The sound reaching a sensor at launch-point distance  $d$  in the far field depends mainly on angle  $\vartheta$  and source range  $r$ . (Not to scale.)

a dimensionless frequency ( $f$ : frequency). As this number varies between 0.004 and 0.4, the peak direction changes from about  $30^\circ$  to about  $60^\circ$  from the jet axis—lower frequencies are preferentially radiated more closely to the jet axis. Far-field spectra in the overall-maximum direction measured after propagation to longer distances are shown in Figure 5.

## NOISE PROPAGATION

From the various sources in the plume, the acoustic emission spreads into all directions. While over- and underpressures are still strong (say, above 0.001 of atmospheric pressure = 100 Pa), nonlinear effects occur: pressure peaks run faster, overtaking and swallowing smaller peaks and valleys, leading to the steep pressure jumps of so-called weak shock that are also more strongly absorbed.<sup>28</sup> Further out, the various mechanisms of linear sound propagation in the atmosphere hold and the various source contributions superpose. In the far field, the system can be treated as a fluctuating point source.

At first a few basics are to be presented: acoustic intensity  $I$  (the area density of power) and sound pressure  $p$  (that is, the difference to static pressure) are related according to

$$I = P_{ac}/A = p^2/(\rho_0 c_S), \quad (6)$$

where the product of static density  $\rho_0$  and low-amplitude sound velocity  $c_S$  is the impedance of free air, about  $400 \text{ kg}/(\text{m}^2\text{s})$ . Eq. (6) holds for the momentary values as well as for the (root-)mean-square (rms) ones that are more often used. The usual logarithmic measure of sound intensity, sound level  $L$ , gives the same values for amplitude as well as intensity, if the respective appropriate reference values are taken: usually,  $I_{ref} = 10^{-12} \text{ W/m}^2$  and  $p_{ref} = 2 \cdot 10^{-5} \text{ Pa}$ . Thus, with Eq. (6),

$$L = 20 \log_{10}(p_{rms}/p_{ref}) = 10 \log_{10}(I_{rms}/I_{ref}). \quad (7)$$

The most important propagation effects are:<sup>29</sup>

Due to *spherical spreading*, the sound pressure  $p$  decreases in proportion to inverse distance  $r$ :

$$p(r) = p(r_0)r_0/r, \quad (8)$$

where the reference distance  $r_0$  is often taken to be 1 m (which is fictitious in the present case). In case of wind of speed  $v_W$ , the effective propagation radius is changed by a factor  $(1 \pm v_W/c_S)$ , for up- and down-wind propagation, respectively ( $c_S$  is the sound speed, about 330 m/s). Because the wind speed is rarely above 30 m/s at the ground, the corresponding amplitude change is far below 10% most of the time (more drastic change is produced by wind shear at longer range, see below).

*Molecular absorption* in the air adds an exponential term:

$$p(r) = p(r_0)(r_0/r)e^{-\alpha(f)r}. \quad (9)$$

Here the absorption coefficient  $\alpha(f)$  increases strongly with frequency  $f$  and depends on temperature, pressure and humidity. At the low frequencies and relatively short distances considered here, absorption is not important.<sup>30</sup>

*Reflection at the ground* is a complicated phenomenon in particular in case of grazing incidence along porous soil; the complex acoustic impedance and a phase change of nearly  $180^\circ$  lead to unusual attenuation at low frequencies.<sup>31</sup> However, in the present case, the source climbs fast so that soon steep angles of incidence apply at which the ground acts as a hard reflector with little phase change, so that the reflected wave adds constructively. For a microphone at finite altitude, the reflected wave (attenuated by the longer path length and reflection coefficient below 1) will result in negative or positive interference at certain frequencies. At the ground level—which is relevant for acoustic-seismic transfer, see below—the amplitude essentially doubles.

*Refraction* of sound waves occurs if there are vertical gradients of temperature or wind speed. Thus the sound speed changes with altitude which causes ray paths to become curved. Normally during the day the temperature decreases with altitude; since the sound speed is proportional to the square root of absolute temperature, sound rays are bent upward. In case of wind shear where the speed practically always increases with height due to the friction at the ground, similar conditions are given for propagation upwind. The opposite case—rays bending downward—exists with a temperature inversion or, in case of a wind gradient, in the downwind direction. Downward bending would not present a problem for detection of rocket launch noise.<sup>32</sup> However, in the case of upward bending the lowest ray from the source that just grazes the ground rises again beyond that (Figure 4), producing a shadow zone where sound can only enter by

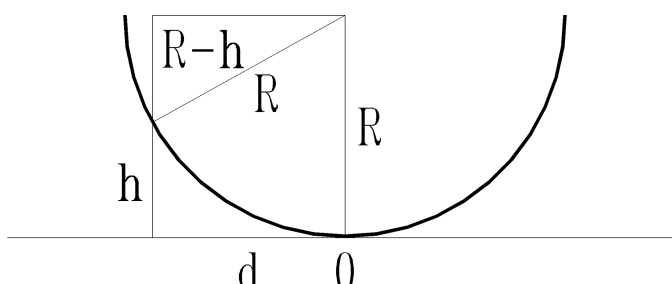


**Figure 4:** Limiting ray (circular for linear decrease of sound velocity with altitude) in case of upward refraction, drawn for a receiver at the ground at zero. Sound from sources on the left hand side on the curve can just reach the receiver. On the right a shadow zone forms below the limiting ray. For sources below the curve the grazing point and the shadow zone shift to the left so that the receiver is in the shadow. The horizontal distance  $d$  for a given altitude  $h$  follows from the rectangular triangle.

other, weaker mechanisms (diffraction, scattering by turbulence). The resulting low amplitude in the shadow region does not pose problems for launch detection, however, since the source is rising so that the shadow zone will form at larger and larger distances. For a rough estimate, one can assume a linear change of sound velocity or wind speed with altitude, then the rays form circles of radius

$$R = c/(\partial c/\partial h), \quad (10)$$

where  $c$  is the sound speed and the constant derivative with respect to altitude  $h$  is approximated from the gradients of temperature  $T$  and wind speed  $\vec{v}$  by

$$\partial c/\partial h \cong 1/2 c/T \partial T/\partial h + \vec{n} \cdot \partial \vec{v}/\partial h, \quad (11)$$

$\vec{n}$  is the unit vector in the propagation direction.<sup>33</sup> With a temperature lapse of 10 K over 1 km and assuming a wind speed increase from 0 at the ground to 200 km/h = 56 m/s in  $h = 10$  km, in the upwind direction the sound-velocity gradient becomes  $\partial c/\partial h \cong -0.012 \text{ s}^{-1}$ , and the radius  $R \cong 28$  km. From Figure 4 one derives that for a specified altitude  $h$  on the circle the horizontal distance  $d$  is

$$d = (2hR - h^2)^{1/2}. \quad (12)$$

Demanding that the sound is to reach the receiver at the ground at least from the time when the vertically climbing missile passes the altitude  $h$ , one gets  $d$  as the maximum distance of the receiver from the launch point. With a circle of  $R \cong 28$  km, for 10 m altitude the maximum sensor distance becomes 0.75 km, for 100 m 2.4 km, and for 1 km 7.4 km. The latter distance is inappropriate because of too low amplitude (see below), so deployment at no more than a few km leaves leeway for stronger gradients while the sensor would still not be in the shadow zone for the overwhelming part of the launch trajectory.

A final effect worth mentioning is *turbulence*. Random fluctuations scatter sound energy. This leads to time-varying multiple paths and increases the fluctuations in a signal, which however in the present case is fluctuating anyway.

(Diffraction and additional effects from the ground shape or plants are less important in the present context.)

Since for the present purpose only rough estimates are needed, one can model the propagation by the simple  $1/r$  decrease with distance and neglect all other effects, keeping in mind that they can introduce deviations by a factor of two or so. This is justified from the distance where linear propagation dominates and when the altitude is above the limiting ray of downward refraction. Spectra taken at launches of the U.S. Peacekeeper ICBM show that frequency-dependent effects are small at least between 0.3 and 1.2 km (Figure 5).<sup>34</sup> At the three distances measured, the overall sound-pressure levels were within 1 dB of the values predicted with linear propagation assuming maximum directivity gain of 8 dB in 70° (smaller missiles showed larger deviations). Since other sources mention maximum angles of 60° or even below, the distance of the maximum has some uncertainty.

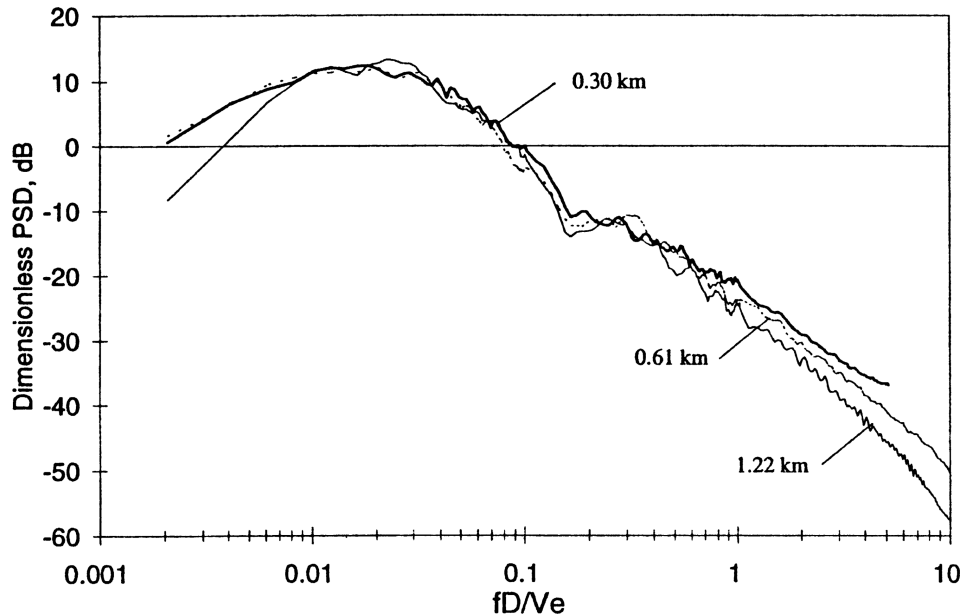


**Figure 5:** Dimensionless estimates of sound power spectral density averaged over the time interval when the measured overall sound-pressure level was within 6 dB (factor 4 in intensity, 2 in pressure) of the maximum, at 0.30, 0.61, and 1.22 km from the launch site for the U.S. Peacekeeper ICBM, plotted versus the Strouhal number  $Sr = fD_e/v$  (see Eq. (5)). With  $D_e = 1.45\text{ m}$  and  $v \approx 2.6\text{ km/s}$ ,<sup>1</sup>  $Sr = 1$  here corresponds to  $f = 1.8\text{ kHz}$ , the maximum is at 30–40 Hz. The average levels during this period were 134.9, 128.2, and 123.3 dB, corresponding to rms pressures of 111, 51, and 29 Pa, respectively. That the values decrease with distance at higher frequencies is probably caused by atmospheric absorption. From McInerny (Note 15), copyright American Institute of Aeronautics and Astronautics 1996, reprinted by permission of AIAA.

<sup>1</sup>  $D_e$  value derived from Table 1 in McInerny (Note 15) where the three absolute distances are also given relative to  $D_e$

To get a feeling for signal strength and time course, a simple model was used where the maximum of the frequency-independent directivity gain was 6 dB (factor 4 in intensity) in  $\vartheta = 60^\circ$ , decreasing to 0 dB at  $40^\circ$  and  $80^\circ$  (inset in Figure 6):

$$I(t_S) = P_{ac} DF(\vartheta) / (4\pi r^2), \quad (13)$$

where the sensor time  $t_S$  lags the source time  $t$  by the propagation delay along the slant distance  $r$ ,

$$t_S = t + r(t)/c_S, \quad \text{and} \quad (14)$$

$$r(t) = h(t) / \sin \vartheta(t), \quad (15)$$

with the rocket altitude  $h(t)$  and the angle to the sensor  $\vartheta(t)$  at time  $t$ . A vertical launch of the model ballistic missile was assumed with  $P_{ac} = 15\text{ MW}$ ; at various

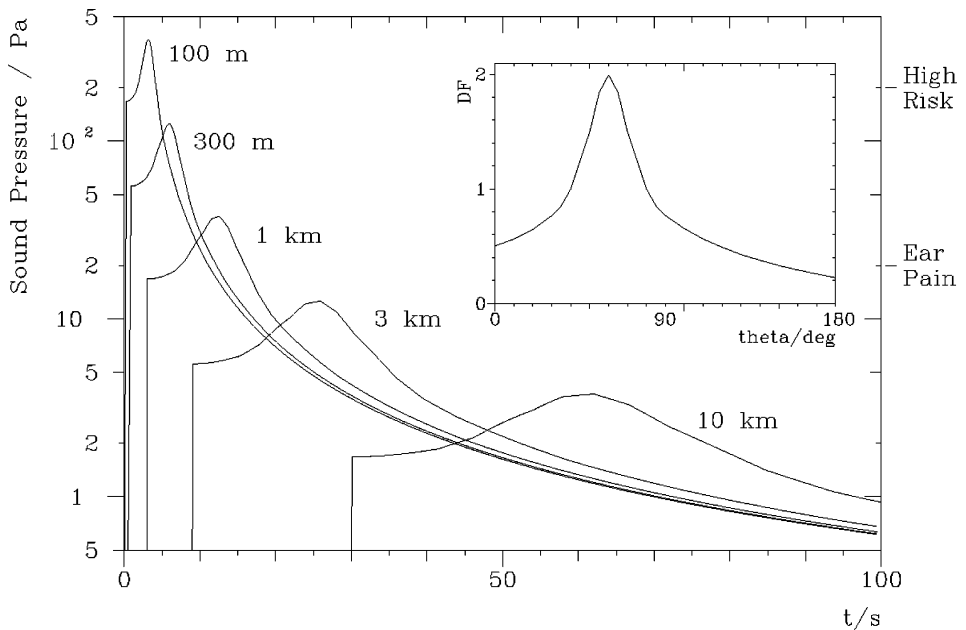


**Figure 6:** Theoretical time course of rms sound pressure at various distances from the launch point for the model ballistic missile with 15 MW acoustic power using a simple model (see text). The duration above half the maximum value varies between 3.2 s (at 100 m) and 36 s (at 10 km). In reality, the starting signal strengths would be lower due to the ground effect at grazing incidence (see Figure 7). As a rule of thumb, ear pain starts at 20 Pa (120 dB re 20  $\mu$ Pa); above 200 Pa (140 dB) even short exposure can cause permanent hearing loss.

sensor-launch point distances, time courses of  $p_{rms}$  following from Eq. (13) with Eq. (6) were computed and Figure 6 shows the results. In real measurements, the signal onsets would be lower due to the ground effect at grazing angle and possibly refraction; later reflection could increase the pressure by up to a factor of 2. At short distances, amplitudes would be higher because of nonlinear effects. Should the neglected effects be included, deviations by a factor 3 to 6 in pressure can be expected.

A real signal of a U.S. Delta rocket, measured 0.46 km from the launch point, is shown in Figure 7. With 1.15 m effective nozzle diameter, 3.1 MN thrust, and 20 MW acoustic power, this liquid-solid rocket is roughly comparable to the Peacekeeper ICBM (15 MW).<sup>35</sup> The amplitude increase is smooth, the amplitude peak seems more asymmetric, but the general appearance is similar to the model result. Using the trajectory model with the Delta data<sup>36</sup> (acceleration roughly half that of the Peacekeeper) and the noise model with maximum factor 4 at  $60^\circ$  as above, a maximum rms pressure at 460 m of 94 Pa (occurring 11.1 s after launch) results, with duration above half maximum of 12.5 s. The measured rms pressure over the maximum 1 s was 64 Pa, duration above half maximum about 8 s; using a factor 6.3 at  $70^\circ$ , 130 Pa had been predicted

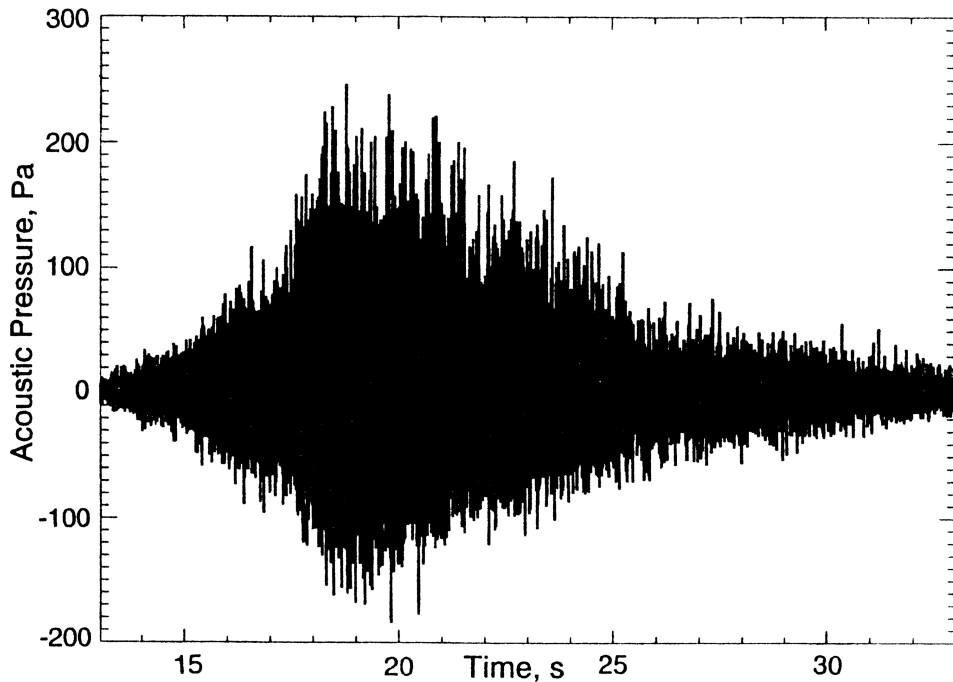


**Figure 7:** Noise measured 0.46 km from the pad during a launch of a U.S. Delta rocket (zero time arbitrary). The signal shows the typical envelope to be expected; the amplitude maximum is produced by the directivity peak pointing towards the sensor. See text. Note that an ICBM may accelerate faster than this space-launch rocket, leading to a shorter signal duration. From McInerney (note 37), copyright American Institute of Aeronautics and Astronautics 1996, reprinted by permission of AIAA.

using the same approach.<sup>37</sup> Thus, the model is roughly correct. An indication of the nonlinear effects (weak shock) in the measured signal is that the positive extremes are stronger than the negative ones. The steep shock fronts resulted in a crest factor of 13 dB during the period when the rms pressure was within 6 dB from its maximum, that is the pressure maximum was 4.5 times the rms pressure. The nonlinear effects become clearer if individual peaks and troughs are resolved, in the derivative, or by special coefficients (beside crest factor, skewness and kurtosis).<sup>38</sup>

## SEISMIC EXCITATION BY LAUNCH NOISE

When an air-pressure variation meets the ground, the force exerted on the latter changes. Since the ground is not rigid, it will deform. The process is very complicated, in particular if nonplane waves and layering are involved as usual. Already for plane waves in a fluid half space overlaying a solid half space, depending on incidence angle, the propagation velocity in the fluid and the velocities of compressional and shear waves in the solid, complex refraction

angles and impedances can occur, corresponding to inhomogeneous waves propagating along the boundary.<sup>39</sup> This case has been used in seismology to treat infrasound-generated surface waves of the Rayleigh type (with elliptical motion in the vertical and propagation directions) in the earth crust where the sound speed is much smaller than the seismic velocities.<sup>40</sup> However, in the uppermost sediment layer at least the shear-wave speed can be below the sound speed in air. In that case, due to the dispersion that occurs with Rayleigh waves in a layered ground, at a certain frequency the phase velocity may equal the apparent sound speed along the ground, so that the seismically propagating excitation superposes constructively with the new air-coupled excitation at each point along its path.<sup>41</sup> Such frequency will be strongly enhanced in the seismic signal. With explosive sources in air, a monofrequency signal starts after the arrival of the air-pressure wave. In the present case of long-duration broadband noise, one expects a strong spectral line. Its frequency depends on the local near-surface layering and the incidence angle; for a rising source, that angle increases, leading to an increase in apparent wave speed along the ground, so that the superposition condition will hold for successively changing (usually, decreasing) frequency.<sup>42</sup>

Acoustic-seismic transfer is particularly strong if the ground is not closed as with rock or ice, but has pores as with the usual sediment. In that case, the air pressure variation at first travels into the pores at very low velocity (tens of m/s) so that due to refraction it propagates practically vertically into the ground. By friction with the grain skeleton, it is strongly attenuated (coefficient of tens of  $\text{m}^{-1}$ ), setting the skeleton into motion. That movement then propagates at much higher velocity under a slant direction.<sup>43</sup> It can be partly reflected at a lower layer boundary and again the surface, contributing to the developing seismic waves, in particular the strongest Rayleigh surface wave. If the latter can be neglected, one speaks of local reaction; the seismic excitation depends only on the local air-pressure variation.

The acoustic-seismic transfer is a linear process; neglecting the complicated theory, it can be described by a simplified equation

$$v_{Srms}(x, y, z) = kp_{rms}(x, y) \quad (16)$$

between the rms sound pressure  $p_{rms}$  acting on the ground at point  $(x, y)$  and the resulting rms soil velocity  $v_{Srms}$  in the depth  $z$  below that point (most often one uses the vertical component). The apparent transfer factor  $k$  is influenced by many circumstances, among them: soil layering, incidence angle, depth, history of excitation before arrival at  $(x, y, z)$ . Due to the frequency dependence of  $k$ , often Eq. (16) is used for the signal component at one frequency.

In silt loam, sand, and loess, frequency-dependent transfer factor values between  $10^{-6}$  and  $10^{-4}$   $\text{m}/(\text{sPa})$  were observed.<sup>44</sup> Figure 8 shows the apparent transfer factors—quotients of seismic over acoustic spectra—from own

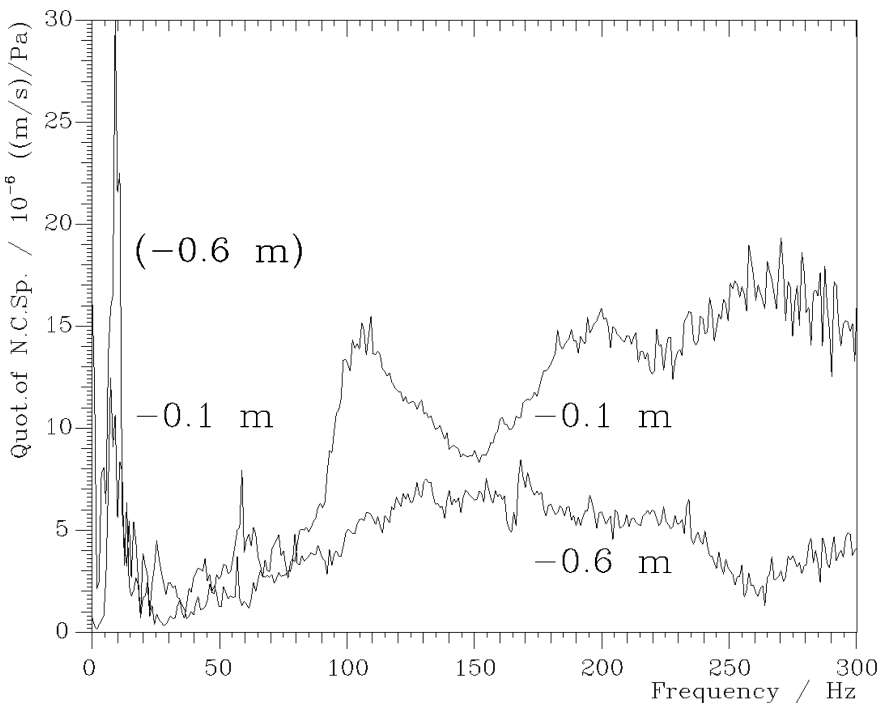


**Figure 8:** Examples of acoustic-seismic transfer factor on flat grassland: quotient of seismic and acoustic amplitude spectrum, at 0.1 and 0.6 m depth (microphones were at 0.3 m altitude), from signals measured 95 and 145 m from the runway center line, respectively, during a take-off of a Tornado fighter-bomber with afterburner. Absolute magnitude of averages over 28 complex quotients from spectra with 87.5% overlap, total duration 4.8 s, around the time of closest approach. The apparent high values around 10 Hz for the -0.6-m geophone are an artifact caused by the 20-Hz lower cutoff frequency of the corresponding microphone (the other one had 2 Hz). Own measurement, Bochum Verification Project, 2 Febr. 1995, former German Air Force Base Jever-Schortens.<sup>1</sup>

<sup>1</sup>The measurements are described and first evaluations of transfer factor were given in R. Blumrich, *Sound Propagation and Seismic Signals of Aircraft Used for Airport Monitoring*, Verification—Research Reports, no. 10, ISL, Hagen (1998). See also R. Blumrich, J. Altmann, "Aircraft Sound Propagation Near to the Ground: Measurements and Calculations," *ACUSTICA—acta acustica* 85 (4) (1999): 495–504.

measurements on a German air force base with grass on sandy soil, using jet-afterburner noise from a taking-off Tornado fighter-bomber as source. As expected, the seismic excitation is stronger closer to the surface. The peak around 10 Hz (absolute value too high for the -0.6-m geophone) is probably caused by a Rayleigh wave traveling in phase with the sound. Also this result shows that for an order-of-magnitude estimate, a transfer factor of  $k \approx 10^{-5}$  m/(sPa) can be used for sediment close to the surface. (Of course, the seismic amplitude and  $k$  are much smaller at larger depth. Deploying seismometers in deep boreholes is the main method of reducing acoustically and wind-produced (and other surface-related) seismic noise in sensitive measurements.<sup>45)</sup>

Intuitively, lower transfer from acoustic pressure to seismic vibration is expected if the ground is hard or overlain by soft material. Limiting cases would be on the one hand, rock, on the other hand, snow cover.

For the case of barren rock where one would expect low coupling due to the harder material and absence of pores, measurements were not found in the literature. The closest is a case designated as “rock outcrop” that however was still overlain by 2 m of clay; here a value around  $1.5 \cdot 10^{-6}$  m/(sPa) was found with sonic booms.<sup>46</sup> The factor may be lower for pure rock without weathered layer on top, however, this case is not very relevant here since ICBM silos are mostly built in sedimentary areas. If missile launches need to be detected by sensors on barren rock, calibrating measurements of the transfer factor could be done easily. Even if the factor were lower than  $10^{-6}$  m/(sPa) by one or two orders of magnitude, reliable detection would still be possible since all other air-coupled vibration would be reduced likewise. As a measure of last resort one could choose a sensor site closer to the silo.

Snow cover, on the other hand, does not change the transfer factor strongly. For 11 different snow types, values between  $2 \cdot 10^{-6}$  and  $1.6 \cdot 10^{-5}$  m/(sPa) were observed.<sup>47</sup> Even though the ground may be harder by freezing and soil pores closed by ice, the porous snow provides a large area for air-ground interaction. However, due to the acoustic softness, the acoustic pressure above snow will be damped more strongly; for horizontal incidence after a range of 200 m about a factor of 10 lower sound pressure and soil velocity were observed.<sup>48</sup> On the other hand, this ground effect should decrease strongly as the source-elevation angle increases in case of a missile launch observed by a sensor at a range below a few km.

## DETECTION AND DISCRIMINATION CONSIDERATIONS

To assess the reliability of a missile-launch detection system, one has to consider the probability of detection and the rate of false alarms. The first has to do with background noise that might arrive via the air or from the ground (electronic noise can be kept below both). False alarms could arise mainly from other strong sources. Seismically, one could think of earthquakes and vehicles passing at close distance; the most plausible acoustic sources are thunder, aircraft and land vehicles. These and others are discussed in the following.

### Acoustic Background

Cultural noise from towns or industry will not be relevant. Sound amplitudes from work, motors, etc. inside the silos will be many orders of magnitude below launch noise. Typical rms values of background sound pressure (bandwidth 3–10,000 Hz) are around  $10^{-3}$  Pa.<sup>49</sup> With the typical value of  $k = 10^{-5}$  m/(sPa) this would lead to negligible soil vibration of  $10^{-8}$  m/s.

## Seismic Background

The usual seismic background is produced by distant earthquakes, ocean waves, meteorological influences, and effects from human activity (traffic, industry, etc.). At remote locations with the sensors coupled to rock, conservative low and high estimates of rms soil velocity in the frequency range 1–100 Hz are  $9 \cdot 10^{-10}$  and  $6 \cdot 10^{-6}$  m/s, respectively.<sup>50</sup> The latter value is probably far too high; at our measurements in sediment with geophones buried at –0.1 m, the rms soil velocity was about  $6 \cdot 10^{-7}$  m/s during the day, and  $3 \cdot 10^{-7}$  m/s during the night (bandwidth 3 to  $> 300$  Hz).<sup>51</sup>

The most important natural source will be strong, varying wind, which however will not lead to significant soil movement if the surface is smooth. In measurements with sparse vegetation, rms soil velocities on the order of  $10^{-7}$  m/s were measured at the highest mean wind speed observed, 10 m/s.<sup>52</sup> Only if there are structures such as trees or masts will considerable forces be exerted on the soil, producing some more vibration. In a forest of about 10 m tall pines, we observed an increased rms velocity of  $1 \cdot 10^{-6}$  m/s (as compared to  $3 \cdot 10^{-7}$  m/s) during a windy and rainy night when the average wind speed (measured at about 14 km distance in 16 m height, outside the forest) was around 5 m/s with a maximum of 11 m/s.<sup>53</sup> Higher values are plausible with stronger wind. Excited by movement of trees or masts, the spectrum will reflect their frequencies, so that it would be clearly different from launch noise. Nevertheless, sensor sites should be chosen so that bushes, trees, masts and the like are at considerable distance (optimally, several hundred m). Objects of smaller height and little wind resistance (a fence, a small satellite antenna) could probably be in the immediate vicinity.

## Earthquakes

Earthquakes produce very strong ground motion near their epicenters: at a few km from the fault plane, acceleration above  $10 \text{ m/s}^2$  was observed, corresponding to velocity above 20 m/s at a dominant frequency of 3 Hz.<sup>54</sup> This is much higher than launch-noise-induced motion even at the launch point (see Figure 11), so that at somewhat larger source distance typical launch amplitudes will be reached. However, at such distance the signal is a short event of a few seconds duration with essentially one strong cycle, with correspondingly dominating frequency below 1 Hz.<sup>55</sup> At longer range, the typical seismic event signal arises with successive arrivals of compressional, shear and surface waves plus various reflected components. (The same holds for explosions.) Both types can be easily distinguished from launch-noise vibration using the signal time course and spectrum. Since ICBM fields are located deep inside the continental plates, close earthquakes are very rare anyway.

## Thunder<sup>56</sup>

In lightning, a plasma channel is formed and heated by the electrical discharge with an energy line density on the order of 0.2 MJ/m; with typical

channel lengths of a few km, around 1 GJ is released. Of this, a few times 0.1% are converted to acoustic radiation; in one study, acoustic energies derived from observed power flux and distance were 1–15 MJ for ground flashes and 2–3 MJ for cloud flashes.<sup>57</sup> The outgoing pressure wave starts as strong shock (overpressure far above ambient air pressure). Geometric spreading and strong absorption then lead to weak shock (over- and underpressure a small part of rest pressure) for which still strong absorption holds. Farther out, the steep pressure jump is smoothed, pressure pulses become rounded, and linear propagation prevails with normal molecular absorption (increasing strongly with frequency, important mainly above 100 Hz), additional frequency-dependent attenuation due to grazing incidence above porous ground, and refraction, as described previously. The plasma channel is tortuous and has branches, in addition it is extended; thus, acoustic waves originated at different parts (essentially simultaneously, arrive at different times at a sensor. Depending on the length and geometry of the channel with respect to the receiver, the travel-time difference from the closest to the most distant part can be above 10 s. Typical durations of thunder are 5–20 s, usually with several amplitude peaks. Spectra are broad-band with peaks from below 4 Hz to 125 Hz. At close range, thunder is short, intense and contains higher frequencies (peals, claps). From far distance, thunder lasts longer, lower frequencies dominate, and amplitudes are weak (rumble). Due to the refraction shadow zone, ranges are normally below 25 km. Using linear spherical spreading with the distance of the first arrival  $r$ , neglecting absorption, the energy area density becomes

$$(E/A)(r) = E_{ac}/(4\pi r^2). \quad (17)$$

The energy,

$$E(r) = \bar{P}(r)\Delta t, \quad (18)$$

is spread over a time interval  $\Delta t$  so that the acoustic intensity  $I(r)$  (=area density of average power  $\bar{P}(r)$ ) and root-mean-square pressure  $p_{rms}(r)$  become<sup>58</sup>

$$I(r) = p_{rms}^2(r)/(\rho_0 c_S) = (E/A)(r)/\Delta t \quad \text{and} \quad (19)$$

$$p_{rms} = [E_{ac}\rho_0 c_S/(4\pi r^2 \Delta t)]^{1/2}. \quad (20)$$

Putting in lower and upper  $E_{ac}$  values of 1 and 15 MJ and durations  $\Delta t$  of 1 and 2 s for 1 km distance, rms pressure values between 4.0 and 22 Pa result, fitting to the statement that at 1 km the pressure is generally less than 10 Pa.<sup>59</sup> At 3 km, with 2 and 5 s, one gets extreme values of 0.84 and 5.2 Pa, and at 10 km, with 5 and 10 s, the pressure span is 0.18 to 0.98 Pa. These values were used to delineate the thunder region in Figure 11. Single pressure peaks in these intervals will of course be higher than these rms values.

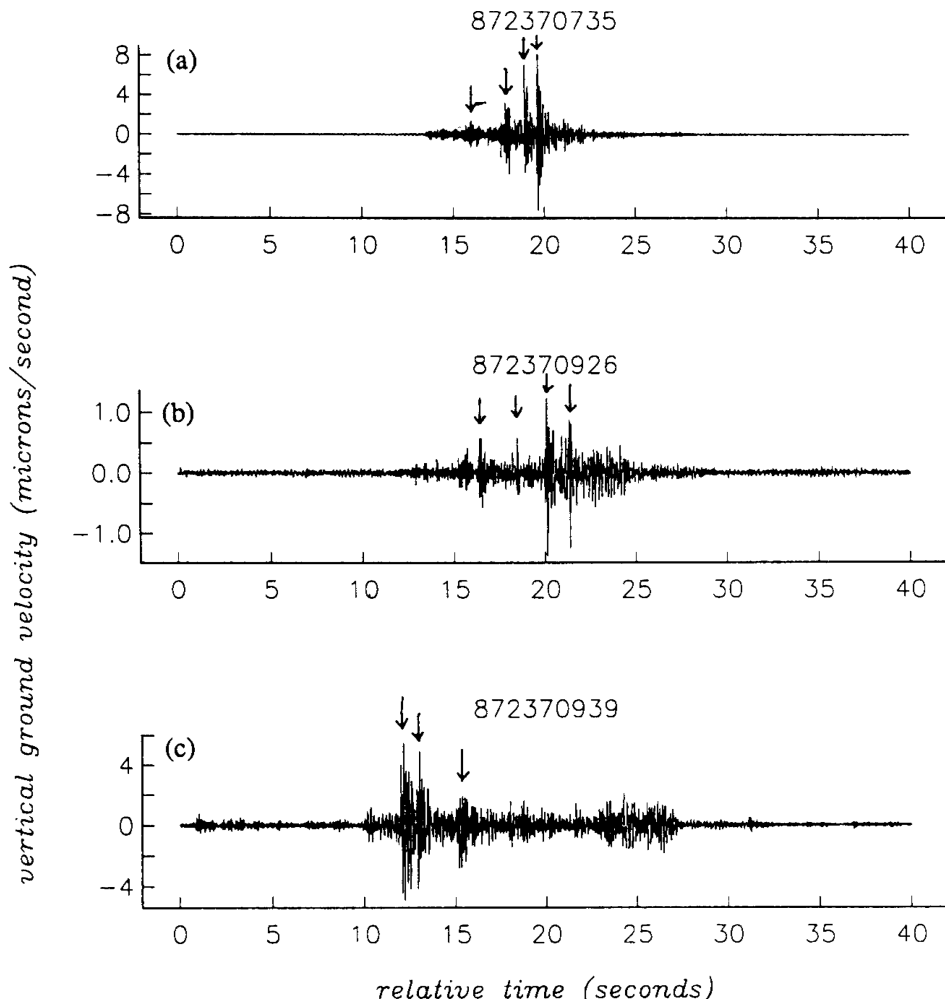


**Figure 9:** Vertical components of ground velocity during three thunder strikes from a thunderstorm approximately 5 km away. Numbers: year, Julian day, time. The signals have irregular envelopes, individual claps can be seen. From Kappus/Vernon 1991 (note 60), copyright 1991 American Geophysical Union, reproduced by permission of American Geophysical Union.

Seismic recordings of three thunder events are shown in Figure 9.<sup>60</sup> They demonstrate that the signal consists of several amplitude peaks. The 13 events observed had maximum amplitudes of  $1\text{--}8 \mu\text{m/s}$  and durations from 5 to 33 s; the thunderstorm was about 5 km away. Since the signals were measured by chance at a seismic station, no acoustic measurements are available. Using Eq. (20) with  $E_{ac} = 10 \text{ MJ}$  and  $\Delta t = 15 \text{ s}$  gives  $p = 0.85 \text{ Pa}$ . Estimating the peak pressure at four times this value and using a medium peak soil velocity of  $5 \mu\text{m/s}$ , the apparent acoustic-seismic transfer factor in the amplitude realm becomes  $1.5 \cdot 10^{-6} \text{ m/(s Pa)}$ . This is lower than typical for porous soil, but fits

the ground structure at the station: granite with a 1 m weathered layer on top, seismometer placed on concrete anchored to the solid granite. Generalizing, one can state that at close distance (less than a few km), thunder signals can be strong but show an irregular envelope with one or more peaks, different from the smooth envelope of a missile launch at ranges below a few km. Thunder from longer distances (rumble) will mostly have an irregular envelope, too, but it may in rare cases appear similar to the one from a launch. The maximum amplitude will be low, however. Analyzing the envelope form and the maximum amplitude should suffice for discrimination. If higher reliability were required, one could add spectral characteristics, look at the propagation delays at the sensors of various silos, or include direction-finding using multiple sensors at each site. Adding an antenna and evaluating the electromagnetic signal from the lightning could be done, too, but does not seem necessary.

## Overflying Aircraft

Even though the air space above ICBM fields will probably be restricted, one cannot rule out (military) aircraft flying there—many fields are built around an air force base. Their noise could only be mistaken for rocket noise if the amplitude is high enough, that is if the altitude is low. Civilian jet airliners are much less noisy and would not fly low except during take-off and landing. Propeller aircraft and helicopters can easily be discarded by looking at the spectrum that, due to the periodic source, consists mainly of harmonic lines.<sup>61</sup> Only jet engines produce the same kind of broad-band spectra. Supersonic flight can also be easily recognized by the typical N wave. It consists of a steep overpressure shock-wave, then about linear decrease to underpressure, followed by another steep increase to normal pressure.<sup>62</sup> For level flight, the duration is given by the length of the aircraft divided by its speed—with 15 m and above 330 m/s, below 50 ms.<sup>63</sup> Broadband noise principally similar to the one from a rocket exhaust is produced by subsonic jet aircraft. This is demonstrated for fighter-bomber over-flights with about 200 m shortest distance in Figure 10; the signal duration, amplitude time course, and the absolute maximum amplitude are comparable at least with the afterburner on. Note however, that the aircraft maximum at 200 m is only about 1/5 of the one at about 500 m source range for the rocket in Figure 7. Comparing with that figure, a more symmetric increase and decrease are evident here. The spectral maximum (here above 100 Hz as opposed to 30–40 Hz in Figure 5) can also give a hint. However, these characteristics do not seem robust enough for discrimination. For a better recognition of low-level subsonic jet aircraft, inclusion of signals from sensors at more locations seems useful. In the case of larger mutual distances, the time sequence of respective amplitude peaks gives an indication if the trajectory was more or less level or vertical. With sensors at close distance, one can gain the direction to the source from the wave phases; for a vertical launch, the azimuth angle is constant

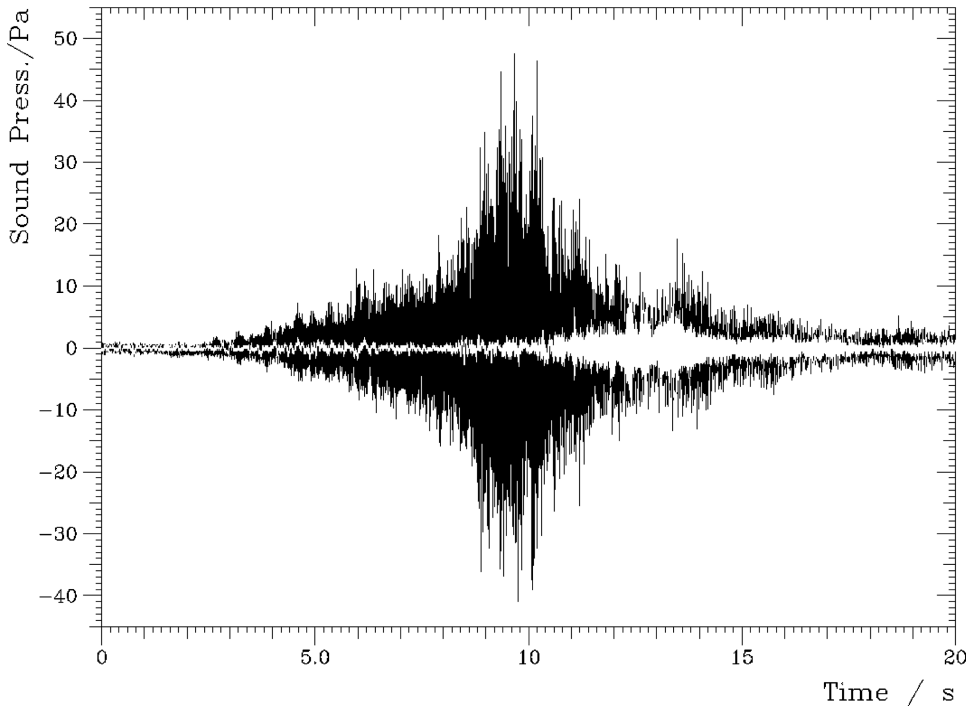


**Figure 10:** Acoustic signal at the ground for subsonic low-level overflights of military jet aircraft. Tornado fighter-bombers flew straight, level trajectories with the point of closest approach at about 200 m slant range. Black: afterburner on, about 140 m/s, passing at 100–150 m horizontal and 150–250 m slant range; white: afterburner off, 110 m/s, passing overhead at 200 m altitude; arbitrary start times. Own measurements, Bochum Verification Project, 2 Febr./31 Jan. 1995, former German Air Force Base Jever-Schortens.<sup>1</sup>

<sup>1</sup>The overflight without afterburner was evaluated in R. Blumrich, J. Altmann, "Medium-range localisation of aircraft via triangulation," *Applied Acoustics* 61 (1) (Sept. 2000): 65–82 (figure 7). For the other overflight triangulation has not yet been done, the speed was estimated using the delay of 1.1 s between the maximums at two microphone arrangements 150 m apart. Probably, the flight occurred vertically above the runway the centerline of which was about 150 m from the microphones. The measurements are described in Blumrich (Note 1 of Figure 8).

whereas for an aircraft it changes with time. (The case of a vertical-take-off jet aircraft taking off close to the sensors is extremely unlikely, but could probably be discriminated by much smaller acceleration and climb speed.)

## Passing Vehicles

Systematic measurements by the Bochum Verification Project have shown that the strongest seismic excitation is produced by tracked vehicles with typical peak soil velocities of several times  $10^{-3}$  m/s at 10 m, and of  $10^{-4}$  m/s at 100 m distance, with a distance decrease stronger than with  $1/r$ ; heavy

trucks are lower by a factor of 30. The acoustic amplitude decreases with  $1/r^{64}$ . Tracked vehicles are not expected in the vicinity of ICBM silos (except maybe in case of civil war). Their seismic signals are quasi-periodic due to the engine sound coupling into the ground and the wheels rolling over the track elements.<sup>65</sup> Thus, the spectrum has strong line components and can be easily distinguished from a launch spectrum. More realistic are trucks; the amplitude time course could principally be similar to the one of a missile launch, if the vehicle would drive with about constant speed along an about linear path, passing the sensor in the appropriate distance. However, also here the seismic spectrum contains dominant lines stemming from the engine that can serve for distinction.<sup>66</sup>

### Synopsis

The amplitudes versus distance of the relevant sources are combined in Figure 11. Shown is the maximum expected rms sound pressure (left ordinate) versus distance (horizontal from launch point for ballistic missiles, slant for the others). Peak values can be higher by a factor 3 to 6. The right ordinate shows the resulting rms soil velocity if a transfer factor of  $k = 10^{-5}$  m/(sPa)

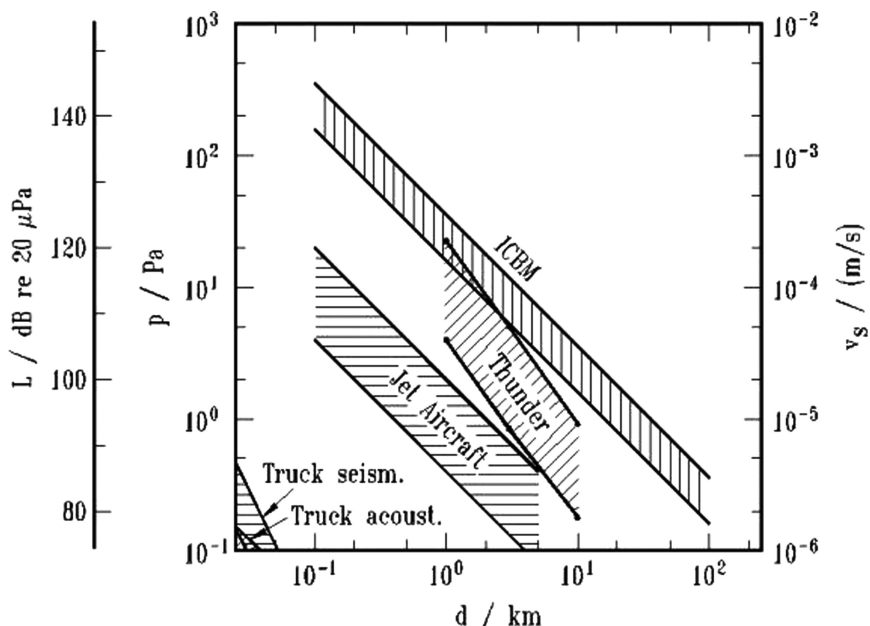


**Figure 11:** Estimates of maximum rms sound pressure versus horizontal distance from the launch point (ICBM) or slant range from the source (others). See text. ICBM, thunder: simple models; jet aircraft, trucks: summary from own measurements. Assuming an acoustic-seismic transfer factor of  $k = 10^{-5}$  m/(s Pa), the sound pressure will give rise to the seismic values of the trucks relate to that scale.

holds; actually, it may differ by a factor 0.1 to 10. Since all acoustic sources would be affected in the same way, the absolute value is not relevant, as long as the amplitude remains high enough above nonacoustically caused seismic noise.

For the ICBM, the simple linear model was used with acoustic powers of 5 and 25 MW (similar to the Minuteman III and clearly above the Peacekeeper, see previous information). At short range, the sound pressure will be higher than shown until the stronger nonlinear absorption will have reduced the pressure jumps. For all sources, at large range, refraction can significantly increase or decrease the pressure. Refraction and the other effects not considered in the model may lead to deviations by a factor 0.3 to 3 between, say, 0.2 and 20 km. Thunder was estimated with a simple model, too, using the values given above. For jet aircraft, typical rms values at 100 m were estimated from our measurements with and without afterburner<sup>67</sup> (see also Figure 10) and extrapolated assuming just geometric expansion. The truck values stem from our measurements, too, for heavy and medium trucks, respectively;<sup>68</sup> the seismic values relate to the right-hand ordinate.

Wind-generated soil movement is on the order of  $10^{-7}$  m/s at smooth terrain without high plants or other structures and maybe a few times  $10^{-6}$  m/s with trees, other seismic background is between  $10^{-9}$  and at maximum a few times  $10^{-6}$  m/s. Conservatively taking  $10^{-5}$  m/s as an upper bound, the launch amplitude would be higher out to a few times 10 km (except in case of upward refraction).

A criterion for the maximum acceptable sensor distance from the ICBM silo can be derived from the two sources next in strength. Even though additional criteria can be used for discrimination, one would want a clear amplitude difference. Is that possible?

For subsonic jet aircraft, a worst-case assumption might be an overflight with afterburner on (upper end of amplitude range) at 30 m altitude, resulting in around 70 Pa rms pressure at maximum. This value is crossed by the low-end ICBM at 230 m, by the high-end one at 520 m. The amplitude factor between ICBM and aircraft required, depends on the probability of such overflights, the missile type, and the reliability of discrimination using other criteria. If one wants a factor of two, the seismic sensor(s) should be no farther than 115 m. However, even then, an overflight at 15 m altitude would create the same maximum rms soil velocity, demonstrating the need to include other criteria anyway. (This is easy in this case; assuming 100 m/s speed, the signal would stay above half of its maximum for only 0.5 s.)

Concerning thunder, signals from short ranges can be stronger than those of a missile launch. However, the former can be recognized by a short duration and possibly several amplitude peaks. Durations of around 10 s with a smooth increase and decrease are only expected for a small portion of distant events.

Taking 5 km as a lower bound for that distance, one arrives at about 3 Pa at the upper margin. Requiring that the launch amplitude is above 10 times that value, the sensor(s) should be closer than about 500 m or 1.1 km from a low- or high-end-ICBM silo, respectively.

Both arguments suggest that the sensor(s) should not be farther than several hundred m up to 1 km. If that is warranted, a truck does not present an amplitude problem even if it passes at 20 m distance. The shorter the distance, the better the discrimination capability by amplitude alone will be; a lower limit will be posed by signals from normal work at the silo, and by the motive to limit intrusiveness. Thus, a sensor distance between 100 m and 500 m seems appropriate.

This has immediate consequences on the number of sensor sites. In order to prevent damage to several silos from one nuclear explosion, ICBM silos have been dispersed widely. For example, in a site diagram of the ICBM base Grand Forks Air Force Base (North Dakota) that probably was given by the USA to the Russian Federation under the START 1 Treaty, the silos are at about 10 km mutual distance.<sup>69</sup> Thus, one sensor site will be needed for each silo. Covering a whole silo group or even a silo field with one sensor is not possible if one insists on unambiguous, strong amplitudes.

## **Additional Information from Multisensor Arrangements**

In order to provide additional information that may be required for reliable discrimination, several seismic sensors at each site could be used instead of only one. This also creates redundancy that can reduce the consequences of single-channel failures. Principally, one can use a combination of three sensors with orthogonal sensitive axes, measuring the three spatial components of ground movement. Its main orientation should be in the vertical plane connecting the source and the sensor, so that the azimuth to the source can be estimated. However, local irregularities in the ground can cause a considerable lateral component, too, rendering this estimate unreliable.

While three-dimensional soil motion gives interesting information and can be evaluated in addition if sensor and processing costs are not extremely limited, the alternative is more promising: using three (or maybe more) sensors that are spread out over a few to several tens of meters. Only the vertical component of ground motion needs to be measured. The speed and direction of ground excitation across such an array can be determined by a cross-correlation method, the maxima providing the time differences between pairs of similar signals arriving at the sensors. From these, one can determine a consistent two-dimensional speed vector that explains the delays. Alternatively, the signals can be summed after applying the negative of the theoretical delays from an assumed speed vector (beam forming). If the area of possible vectors is covered, the correct one will show up in the strongest sum signal because here all sensor

signals superpose coherently. Both methods yield the azimuth to the source and the apparent wave speed  $v_G$  along the ground. Since for a sound-caused signal

$$v_G = c_S / \sin \vartheta, \quad (21)$$

where the wave-incidence angle with the vertical is the same as the emission angle from the plume axis  $\vartheta$ , the elevation angle to the source ( $= 90^\circ - \vartheta$ ) can be estimated. If the source is a missile from the neighboring silo, the horizontal distance is known so that the trajectory can be determined in three dimensions up to an altitude of several times the silo-sensor distance. Higher accuracy is possible if air temperature and the wind vector are measured and included. However, they are probably not needed to confirm a source moving vertically (constant azimuth, increasing elevation) with about constant (slowly increasing) acceleration.

The recommended array size can be estimated from the consideration that the signal at one sensor should change considerably in phase while the wave moves to farthest one; if one demands  $180^\circ$  or  $\pi$ , then the distance should be above half the wavelength of the signal component used. Conversely, if ambiguities from multiple waves fitting into the distance are to be avoided, the minimum distance should be below one wavelength. Looking at frequencies  $f$  between 20 and 100 Hz and apparent wave speeds  $c_G$  between 330 m/s (horizontal propagation) and 730 m/s ( $63^\circ$  elevation, altitude = 2\*sensor-silo distance), along-ground wavelengths  $\lambda_G = c_G/f$  between 3.3 and 37 m result. In the simplest case of three sensors in an equilateral triangle, the spacing should thus be between 2 and 40 m. The appropriate value depends also on the sampling rate  $f_s$  of the digitized signals; without special measures, the smallest delay time that can be determined is one sampling period  $T_S$ . The variation of delay with angle is smallest immediately after launch, around  $\vartheta = 90^\circ$ . With  $T_S = 5$  ms and  $d = 2$  m, the first delay step occurs only when the missile has risen to an elevation angle of  $80^\circ$  ( $\vartheta = 10^\circ$ ); with 1 ms and 40 m, this happens already at  $7^\circ$  elevation. Thus, the latter values are preferable. An upper limit on the sensor spacing is given by the requirement of coherence between the signals; since the source is extended, at least at 100 m silo-sensor distance (that is, around 120 m slant distance at the position of maximum directivity factor), 40 m spacing may be too high. This is an argument to rather go toward the upper end of the possible sensor-distance range, that is, to 300–500 m.

## Probability of Detection, False-Alarm Rate

Quantitatively estimating receiver-operating characteristics (ROC) is difficult at the present stage. Using the criterion of a strong amplitude at close distance, there is no doubt that all missile launches can be detected. However, in order to discriminate against potential other sources that could create false alarms, some events need to be discarded using additional criteria such as

amplitude time course and spectral characteristics (see next section), this goes beyond the usual considerations about ROC curves. By careful design, it seems possible to move the probability of detection arbitrarily close to 1.

Concerning false alarms, one would want a rate below 1 in many decades. To ensure this, one should estimate the probability that thunder from 1 km or closer produces a launch-like amplitude envelope and spectrum—presumably, it is extremely low. One should also investigate whether a jet aircraft—maybe by flying a special maneuver (dive, near-vertical climb?)—can do the same; it seems unlikely that it can.

## SYSTEMS ASPECTS

### Station Design

The cooperative seismic monitoring and early-warning system should have the following characteristics: At 200–500 m distance (for heavy missiles, up to 1 km) from each of the 510 US<sup>70</sup> and 301 Russian<sup>71</sup> ICBM silos an array of at least three vertically sensitive seismic sensors is deployed with a spacing of 20–40 m. The sensors are buried at 0.1–1 m depth and connected to a digitizing, recording and processing system close by that can also be buried; the latter is connected to a communication link. At each sensor site, the only above-ground object would be the (satellite) antenna, possibly a solar panel for power supply, and a fence, if needed. Some protection of the buried components is required (e.g., plowing and digging has to be prevented.)

Wherever possible, the sensors should not be deployed in the line of a close aircraft runway. They should stay away (at least 100 m) from a road. Considerable distance (several 100 m) should be kept from trees, masts, and so on that could couple wind-induced motion into the ground.

With peak soil velocity up to  $10^{-2}$  m/s (see Figure 11), a missile launch creates strong ground motion. For measuring this, accelerometers are more appropriate than the very sensitive seismometers/geophones where the output voltage is proportional to soil velocity. If the sound pressure is about constant over a frequency range, as around the maximum in a launch spectrum (see Figure 5), the soil velocity will also be constant (if the transfer factor  $k$  is about constant). Since acceleration is the time derivative of velocity, accelerometers in this case show a signal that increases with frequency. Assuming 100 Hz as a representative upper frequency, acceleration can reach several  $\text{m/s}^2$  peak.

The dynamic range to be recorded depends on requirements on sensing the background. In soil velocity, the strongest peaks to be expected at the lowest proposed distance of 100 m are at 2 kPa sound pressure (=6\*300 Pa rms for a heavy missile, see Figure 11), corresponding to 0.02 m/s soil velocity with the standard transfer-factor value of  $10^{-5}$  m/(sPa)). If the usual seismic background is to be resolved nearly all the time, the digitization step in velocity should be on

the order of  $10^{-7}$  m/s, that is the dynamic range should be  $2 \cdot 10^5$ , corresponding to 106 dB or 19 bits bipolar linear resolution.<sup>72</sup> Factoring in  $2\pi f$  for acceleration, in the worst case the background would have 1 Hz as main frequency  $f$ , whereas the launch signal might be still strong at 100 Hz—increasing the dynamic range by a factor 100 or adding 6.6 bits of resolution for a total of 25 bits. (At 1 km from the silo, all values would be lower by a factor 1/10 corresponding to -20 dB and -3.3 bits.) A different approach would not care about the background and any signal that is lower in amplitude by at least three decades in amplitude (60 dB), corresponding to 11 bits resolution. By this, one would filter out practically all of the low-amplitude signals that will occur regularly but have nothing to do with a launch. The sensor station would just sense and transmit zero nearly all the time.<sup>73</sup> However, one may want a higher resolution to check the functioning of the sensor and system by exactly these signals, and the record of the background amplitude—averaged over, say, one minute, one hour and one day—can give useful information on the system. Of course, this has to be balanced with the need for secrecy about operations at the silo.

For evaluations that determine the spectral maximum, the high-frequency cutoff should be at 300 Hz or above (see Figure 5 where the maximum is at 30–40 Hz). With the Nyquist condition and some leeway, a sampling rate around 1 kHz for each channel is needed—not demanding for present digital systems.

## Signal Processing and Storage

The processing unit should do the following: Monitor the signal amplitudes continuously, compute and record/transmit the rms averages. Whenever one of the amplitudes crosses an alert threshold, set at about 1/10 of the expected maximum value during a launch, an event is generated; all signals (including at least 10 s pre- and post-event portions, using ring buffers) are stored and processed to arrive at a recognition of event type.

A missile launch can be recognized by the following criteria: (more or less) smooth increase, then decrease of signal envelope with maximum rms value and duration between half-maximum points fitting to missile type and silo-sensor distance (maximum 100–500 Pa at 100 m, 10–50 Pa at 1 km—the exact value is not important; duration about 3 s at 100 m, 5–10 s at 1 km). Computed spectra (corrected for the frequency dependence of the acoustic-seismic transfer factor) are broad band, with one broad maximum at several tens of Hz. The azimuth and elevation time course derived from the sensor array fits to a source starting at the silo and accelerating vertically. With modern fast computers, this processing should take no more than a few seconds, so that the information is available for transmission 20–30 s after the start of the launch.

If the characteristics do not fit to a launch, the event should be classified using appropriate criteria for envelope time course and spectral shape (in part mentioned previously) into the categories: supersonic jet aircraft, subsonic jet

aircraft, propeller aircraft, helicopter, heavy land vehicle, thunder, other. It is probable that over time the “other” category will give rise to additional investigations and maybe introduction of new categories (farmer’s harvester? earthquake?).

With an amplitude threshold at 1/10 of the maximum of a launch, events would be triggered only very rarely—probably fewer than once per month. Continuous functioning of the sensor station would be confirmed on the one hand by transmission of authenticated codes after self-checks at regular intervals—about every minute—on the other hand by transmission of summary information on the actual rms averages.

The characteristics of all events should not only be transmitted, but also stored in a list. The raw data of the most recent events should be stored as well. Also the rms averages should be kept for a reasonable period of time. All three types of information should be retransmitted on request.

## **Calibration**

After the seismic sensors have been buried and a station is set up, the local acoustic-seismic transfer factor  $k$  with its frequency dependence should be estimated using microphones at ground level and a calibrating sound source. Since the ground response is linear up to launch amplitudes, that source can be much weaker. Purely local effects can be taken up by a closeby loudspeaker emitting white noise; excitation of a synchronous Rayleigh wave can be studied with a small bang (firecracker) ignited at about 100 m distance towards the silo, optimally at various elevation angles.<sup>74</sup> Because some variation of the acoustic amplitude and the transfer factor is expected, that is, due to weather (wind, water in soil, snow), 10–20% accuracy will suffice.

## **Communication**

The communication link to the early-warning center of the other party should be independent from the national telecommunication network. Probably, one satellite link for each sensor site is best in terms of cost, intrusiveness, and noninterference; installing directional radio links or cables across a missile field of several hundred km extension with one or a few central satellite stations may turn out more expensive. The communication network should be secure, with authenticated and possibly encrypted messages. It can follow the examples developed in the U.S.-Russian cooperative programs on materials protection, control and accounting.<sup>75</sup>

## **Spoofing**

Whereas a system using microphones could be deceived easily by loudspeakers in the immediate vicinity, setting the ground into motion, in particular with a broadband spectrum up to several hundred hertz, is not easy. There would be no motive to simulate a missile launch, since this could have very

dangerous consequences. Principally one might try to compensate the launch-caused ground motion by excitation with the opposite local phase. Probably, one vibrator (or maybe a high-power loudspeaker in a closed chamber covering tens of m<sup>2</sup> of soil) would be needed for each seismic sensor. Preparations would show up in irregular high signals if such sources are brought close to the sensor sites. Furthermore, excitation at one sensor may lead to components at a neighboring one that would not occur with one strong source at a distance. As an additional precaution, one could deploy a sensor at considerably larger depth (10 m or more) that would need excitation at high power over an even larger area to reach the signal level from a launch. Here, some additional quantitative study is needed.

Cutting the communication link would be sensed immediately if authenticated status signals are transmitted periodically. Digging up of the sensors would produce irregular strong signals that would trigger an inspection request.

### **Sensors, Costs**

As sensors, strong-motion accelerometers are recommended. One possible type is Episensor ES-U (uniaxial) or ES-T (triaxial) from Kinematics Inc., U.S.A., with signal bandwidth from DC to 200 Hz and dynamic range above 140 or 155 dB, respectively. The cost is about \$1,400 and \$3,700, respectively. The same firm offers a low-power digitizing and processing unit Q 330 with an analog-digital converter of 24 bit resolution, with serial telemetry and TCP/IP network connections; with six channels it costs about \$9,600.<sup>76</sup> The maximum selectable sampling rate of 200 Hz (maximum signal frequency below 100 Hz) is not optimum, however. Maybe it could be increased to 0.5 kHz for the mentioned sensors, or to 1 kHz for ones with 400 Hz cut-off frequency, while sacrificing a few bits of resolution. Since the main spectral power of launch noise is below 100 Hz, one can probably also work with 100 Hz cut-off frequency, in order to use commercial off-the-shelf equipment. In that case, the spectral maximum may be less distinct, requiring some change of the spectral-form criterion.

With three sensors, one recording/processing unit, cabling and power supply the cost of one sensing station would be around \$20,000; adding cost for the communication link, installation, and software, the total investment cost for one site will probably lie below \$50,000.

### **CONCLUSIONS AND RECOMMENDATIONS**

An array of three seismic acceleration sensors buried slightly below the surface a few hundred m from an ICBM silo can reliably detect a missile launch and discriminate it from other events that cause strong ground motion. One such array together with a secure communication link to an early-warning center of the other side should be set up at each ICBM silo in the partner countries.

First stations can be installed relatively soon. Actual design can begin immediately, incorporating results of some more concrete investigations that could go on in parallel. Such work could be done in the following areas:<sup>77</sup>

- Calculate acoustic propagation using sophisticated programs that include atmospheric effects such as refraction and reflection at porous ground; in particular, worst-case wind-shear situations could be tested.<sup>78</sup> Detailed plume-noise models may be helpful.<sup>79</sup>
- Determine the best array size for given soil conditions and silo-sensor distance. Study if inclusion of three-dimensional soil movement would improve the discrimination capability markedly.
- Analyze if launch-like seismic signals could be produced by other sources (e.g., a jet aircraft flying a special trajectory) and if so, devise methods to discriminate against them.
- Estimate the probability that thunder causes a signal similar to that of a launch.
- Investigate the potential of spoofing by acoustic or seismic sources close to each sensor; if needed, devise countermeasures.
- Test the ground motion caused by a satellite antenna, a solar panel and a fence in strong wind; if needed, find ways to reduce it.

After a few months of design, selection of hardware and software components, and writing the programs for signal processing and source discrimination, test stations should be installed at a few silos as well as at sites of missile test launches. At the silos, one would gain knowledge on the background around the year, during various weather conditions. At the second, one could test the launch-recognition algorithm. At both, the signal processing and communication links would be tested.

After one or two years, the design can be improved and stations can be deployed at all silos, together with the setting up of the final early-warning centers. Similar systems could be set up in other nuclear-weapon states.

If the experiences with the silo-based systems are positive, one can start considering inclusion of mobile ICBMs. Here the task would be to sense a launch reliably while not giving away the locations of the launcher vehicles beforehand. Acoustic-seismic detection would work if the vehicles are limited to launch regions; the regions would be covered with a grid of sensors every 1–2 km while making sure that the sensitivity would only suffice to detect a vehicle at below 50–100 m distance. The borders of the regions could be monitored by vehicle-sensitive seismic sensors deployed at about 100 m spacing.<sup>80</sup> Simpler and cheaper, but also more intrusive, would be the alternative of launch sensors (contact switches, infrared sensors etc.) on the vehicles that would only communicate when back in garrison except if and when a launch is taking place.<sup>81</sup>

This would leave the problem of submarine launches of ballistic missiles; the latter have become very accurate and can have short flight times from forward positions. Due to the vast areas of ocean and seas and the complexity of underwater sensors, coverage by hydroacoustic sensors is impractical. Similarly to mobile ICBMs, seals with sensors could be mounted on the submarines; on opening of a missile hatch or other preparations for a launch, buoys would be released to the surface (as in a concept to monitor the pulling back of the submarines from forward positions)<sup>82</sup> that would then transmit to satellites. Agreement on such a system would be difficult to achieve.<sup>83</sup>

Since silo locations are fixed and known, monitoring them cooperatively should be much easier to negotiate, in particular if the sensors are deployed at some distance as recommended here. The costs will be very low. The investment cost for one silo (below \$50,000) is much below the value of the missile (tens of millions of \$), and of course lower by additional orders of magnitude than the damage that the missile can cause (up to hundreds of billions of \$, not to mention the deaths). The total system for about 500 U.S. and 300 Russian silos would cost around \$40 million. This compares favorably with the cost of launching six already built Russian early-warning satellites that the U.S. Congressional Budget Office had estimated at \$160 million.<sup>84</sup> With 800 stations, the system would have more than double the number of sensor sites of the International Monitoring System that the Provisional Technical Secretariat of the Comprehensive-Test-Ban-Treaty Organisation (CTBTO) in Vienna operates (321).<sup>85</sup> Different from the latter, the early-warning system uses only one signal type and is concentrated on very few small areas that are monitored by sensors on site. Thus the question of investigating suspicious events is easier by several orders of magnitude. Correspondingly, the personnel requirements and operating cost of the system and two (joint or separate) early-warning centers should be much below those of the CTBTO (2003: about 270 staff, about \$90 million budget, including \$30 million for buildup of the monitoring system).<sup>86</sup>

The cooperative acoustic-seismic early-warning system should not be seen as a surrogate for satellites and space radars. Rather, it should complement those, providing an additional channel of checking whether an attack is actually underway if one system shows suspicious indications. By providing additional reliable information that a launch has not occurred, and by the cooperation that such a system will entail, acoustic-seismic monitoring of ICBM silos can build confidence that may lead to extension to other ballistic missiles and may alleviate further nuclear reductions in the future.

## NOTES AND REFERENCES

1. P. Podvig, "History and the Current Status of the Russian Early-Warning System." *Science and Global Security* 10 (1) (2002): 21–60; see also G. Forden, P. Podvig, T. Postol, "False alarm, nuclear danger—The radar and satellite networks meant to warn Russia of

the imminence of a missile attack are breaking down, heightening the risk of accidental nuclear war." *IEEE Spectrum* 37 (3) (March 2000): 31–39.

2. Between Jan. 1979 and June 1980, four false alarms in the USA were considered serious enough so that a so-called threat assessment conference was called, International Foundation for the Survival and Development of Humanity, *Reducing the Dangers of Accidental and Unauthorized Nuclear Launch and Terrorist Attack: Alternatives to a Ballistic Missile Defense System*. International Foundation for the Survival and Development of Humanity, San Francisco, CA (Jan. 1990). In 1995 a Norwegian high-altitude research rocket was mistaken as Trident submarine-launched nuclear ballistic missile and President Yeltsin was informed, Forden/Podvig/Postol (Note 1).
3. B. G. Blair, H. A. Feiveson, and F. N. von Hippel, "Taking Nuclear Weapons Off Hair-Trigger Alert." *Scientific American* 277 (5) (Nov. 1997): 74–81.
4. G. Forden, *Reducing a Common Danger—Improving Russia's Early-Warning System*. Policy Analysis no. 399, Cato Institute, Washington DC (May 3, 2001), [<http://www.cato.org/pubs/pas/pa399.pdf>] (March 11, 2004).
5. D. E. Mosher, L. H. Schwartz, D. R. Howell, and L. E. Davis, *Beyond the Nuclear Shadow—A Phased Approach for Improving Nuclear Safety and U.S.—Russian Relations*. MR-1666, RAND, Santa Monica, CA (2003).
6. "Clinton/Yeltsin on Exchange of Info on Missile Launches." *USIS Washington File* (Sept. 2, 1998), [[http://www.fas.org/news/russia/1998/98090215\\_tpo.html](http://www.fas.org/news/russia/1998/98090215_tpo.html)] (Febr. 9, 2004).
7. Mosher et al. (Note 5), Chapter 4 (option 2), Chapter 5.
8. See R. L. Garwin, "Space-Based Defenses Against Ballistic Missiles." *Proc. AAAS Annual Meeting Symposium* (Febr. 8, 1992), [<http://fas.org/rlg/920208-space.pdf>] (Febr. 14, 2004); R. L. Garwin, "Post-START: What do We Want? What Can We Achieve?" Testimony to the Committee on Foreign Affairs, United States Senate, February 27, 1992, [<http://fas.org/rlg/022792.htm>] (Febr. 14, 2004).
9. International Foundation (Note 2).
10. E. Velikhov, N. Ponomarev-Stepnoi, V. Sukhoruchkin, *Mutual Remote Monitoring*. Kurchatov Institute, Moscow (1999).
11. Mosher et al. (Note 5), Chapter 4, option 2.
12. This would apply less for (infrasound-capable) pipe-microphone arrangements extending over tens of meters which are used to monitor for atmospheric nuclear explosions over thousands of km under the Comprehensive Test Ban Treaty, [see <http://www.ctbto.org>], Verification Regime, Overview (Feb. 24, 2005). A new type can even be buried under 20 cm of coarse gravel, see M. A. Zumberge et al., "An Optical Fiber Infrasound Sensor: A New Lower Limit on Atmospheric Pressure Noise Between 1 Hz and 10 Hz." *Journal of the Acoustical Society of America* 113 (5) (May 2003): 2474–2479. Using a sensor of 89 m length, the authors have detected a rocket launch at 396 km distance, the amplitude of about 0.5 Pa (0.1–10 Hz) probably resulting from the Mach cone of first-stage reentry (see Section 2, Typical trajectory, below). Because of 20 minutes sound-propagation time, such a distance would not be acceptable for early warning of attack, and reliable discrimination from other low-amplitude events is questionable. Whether buried infrasound sensors would be useful for launch detection at closer range (hundreds of meters near individual silos or tens of km to cover several silos with one sensor (see Section 5, Synopsis, below), deserves a separate study. The installation requirements may turn out similar to the scheme using seismic sensors, the maintenance effort may be higher.
13. G. P. Sutton, *Rocket Propulsion Elements* (Wiley, New York, 1986).

14. See e.g., J. Varnier, "Experimental Study and Simulation of Rocket Engine Freejet Noise." *AIAA Journal* 39 (10) (Oct. 2001): 1851–1859 and refs.
15. S. A. McInerny, "Launch Vehicle Acoustics Part 1: Overall Levels and Spectral Characteristics." *Journal of Aircraft* 33 (3) (May-June 1996): 511–517.
16. Sutton (Note 13), pp. 263f.
17. Using the propellant mass of  $m_p = 20,789 \text{ kg}$  and burn time of 52.6 s, a somewhat different average  $\dot{m} = 395 \text{ kg/s}$  results. In the present context, such differences do not matter.
18. Peacekeeper (MX) ICBM Technical Specifications, [[http://www.geocities.com/peacekeeper\\_icbm/specs.htm](http://www.geocities.com/peacekeeper_icbm/specs.htm)] (Sept. 16, 2004) (first-stage fuel mass 45,300 kg, burn time 56.5 s).
19. Peacekeeper Specifications (Note 18) give 282 s as specific impulse. On the other hand, Sutton (Note 13), p. 293, gives 265 s as upper limit of the  $I_{sp}$  range for solid-fuel rockets. Both statements would be consistent if the 282-s value would refer to vacuum. In that case, from Eq. (1) at sea level (SL) and high altitude one can derive  $I_{V\text{ac}} - I_{s\text{SL}} = p_0 A_e / (g m) = 21 \text{ s}$  with  $p_0 = 101 \text{ kPa}$ ,  $A_e = 1.66 \text{ m}^2$ ; thus,  $I_{s\text{SL}} = 261 \text{ s}$ , and  $v_e = 2.56 \text{ km/s}$ . This would lead to a lower thrust of  $F = 2.05 \text{ MN}$  and kinetic power around 2.5 GW. Since deviations by 10 or 20% in acoustic power do not matter, I have left this question open. In the trajectory calculations I have used 261 s, see note 1 of Figure 1; as acoustic power, I have used 15 MW, see Figure 6.
20. Sutton (Note 13), p. 14, 196; the specific impulse of the Space-Shuttle solid-rocket boosters at sea level is 242 s, in vacuum 268.6 s, see "Countdown! NASA Launch Vehicles and Facilities." PMS 018-B (October 1991), Section 2, NASA Facts Online, Kennedy Spaceflight Center, [<http://www-pao.ksc.nasa.gov/kscpao/nasafact/count2.htm>] (Febr. 4, 2005).
21. Due to the acceleration, Mach waves produced at different times can even superpose in a small area, leading to a "focus boom" there. See e.g., *Final Supplemental Environmental Impact Statement for the Evolved Expendable Launch Vehicle Program*. U.S. Air Force (March 2000), App. U, Section 4, [available at <http://fas.org/spp/military/program/launch/eelv-eis2000>] (July 15, 2003).
22. E.g., W. L. Donn, E. Posmentier, U. Fehr, N. K. Balachandran, "Infrasound at Long Range from Saturn V, 1967." *Science* 162 (3858) (Dec. 6, 1968): 1116–1120; K. L. McLaughlin, A. Gault, D. J. Brown, "Infrasound Detection of Rocket Launches." *22nd Annual DoD/DoE Seismic Research Symposium*, New Orleans LA, 2000, [available via <http://www.rdss.info>] (seismic research) (Febr. 3, 2005), and refs. given there. Similarly, supersonic aircraft such as the Concorde have been detected at large distances at infrasound frequencies, low amplitude and strongly dependent on stratospheric conditions. See e.g., A. Le Pichon, M. Garcès, E. Blanc, M. Barthélémy, D. P. Drob, "Acoustic Propagation and Atmosphere Characteristics Derived from Infrasonic Waves Generated by the Concorde." *Journal of the Acoustical Society of America* 111 (1, Pt. 2) (Jan. 2002): 629–641. For seismic measurements, see e.g., W. L. Donn, I. Dalins, V. McCarty, M. Ewing, G. Kaschak, "Air-Coupled Seismic Waves at Long Range from Apollo Launchings." *Geophysical Journal of the Royal Astronomical Society*, 26 (1–4) (Dec. 1971): 161–171.
23. The global monitoring system of the Comprehensive Test Ban Treaty Organization is not suited for the task: e.g., in North America there are only three infrasound stations (in Manitoba, Alaska, California) [<http://www.ctbto.org/>], Verification Regime, Monitoring Facilities (July 14, 2005). Even though they would occasionally detect a missile launch, this would be unreliable and—with around an hour propagation delay—too late for early warning.

24. C. K. W. Tam, "Jet Noise Generated by Large-Scale Coherent Motion." H. H. Hubbard (ed.), *Aeroacoustics of Flight Vehicles—Theory and Practice, vol. 1, Noise Source*. (Acoustical Society of America, Woodbury NY, 1995)
25. E.g., McInerny (Note 15); J. Varnier, "Experimental Study and Simulation of Rocket Engine Freejet Noise." *AIAA Journal* 39 (10) (Oct. 2001): 1851–1859, and respective refs.
26. McInerny (Note 15) estimates the maximum at  $(L_C + L_S)/2$ , that is rather at 1.3  $L_C$ .
27. One formula for the supersonic core length is  $L_{SC} = D_e(5.22 M_e^{0.9} + 0.22)$ , where  $M_e = v/v_s$  is the Mach number of the exhaust flow, and  $v_s$  is the sound speed in the hot jet; laminar and supersonic core must not be confused, Varnier (Note 25). Note that, e.g., at  $T = 2000$  K,  $v_s$  is  $(2000\text{ K}/293\text{ K})^{1/2}$  times the sound speed at 293 K, i.e., 890 m/s instead of 340 m/s.
28. E.g., O. V. Rudenko, S. I. Soluyan, *Theoretical Foundations of Nonlinear Acoustics*. (Consultants Bureau: New York/London, 1977).
29. E.g., T. F. W. Embleton, G. A. Daigle, "Atmospheric Propagation." In H. H. Hubbard (ed.), *Aeroacoustics of Flight Vehicles—Theory and Practice, vol. 2, Noise Control*. (Acoustical Society of America: Woodbury NY, 1995).
30. E.g., at 40 % relative humidity, 20°C and 98 kPa  $\alpha(100\text{ Hz}) = 5 \cdot 10^{-5}\text{ m}^{-1}$ , i.e. attenuation to 1/e = 0.37 occurs in 20 km. At 10 Hz,  $\alpha$  is 100fold smaller. See Figure 1 in Embleton/Daigle (Note 29).
31. E.g. T. F. W. Embleton, J. E. Piercy, N. Olson, "Outdoor sound propagation over ground of finite impedance." *Journal of the Acoustical Society of America* 59 (2) (Feb. 1976): 267–277; K. Attenborough, "Review of Ground Effects on Outdoor Sound Propagation from Continuous Broadband Sources." *Applied Acoustics* 24 (4) (1988): 289–319.
32. Downward bending in the high atmosphere with reflection at the ground, potentially repeatedly, is the mechanism for detection of sonic booms at very large range, see Note 22.
33. T. Hidaka, K. Kageyama, S. Masuda, "Sound Propagation in the Rest Atmosphere with Linear Sound Velocity Profile." *Journal of the Acoustical Society of Japan (E)* 6 (2) (April 1985): 117–125; G. A. Daigle, T. F. W. Embleton, J. E. Piercy, "Propagation of Sound in the Presence of Gradients and Turbulence Near the Ground." *Journal of the Acoustical Society of America* 79 (3) (March 1986): 613–627.
34. McInerny (Note 15).
35. McInerny (Note 15). Note that the actual launch time is unknown, S. A. McInerny (personal communication).
36. Partly estimated, based on information on Delta 7920/7925 in "Delta 7000." *Encyclopedia Astronautica*, [<http://www.astronautix.com/lvs/dela7000.htm>] (Nov. 16, 2004).
37. McInerny (Note 15), Table 1 (predicted value scaled back from 1 km), duration above half maximum estimated from S. A. McInerny, "Launch Vehicle Acoustics Part 2: Statistics of the Time Domain Data." *Journal of Aircraft* 33 (3) (May-June 1996): 518–523, figure 1 (reproduced as Figure 7 here).
38. McInerny (Note 37). See also S.A. McInerny et al., "The Influence of Low-frequency Instrumentation Response on Rocket Noise Metrics." *Journal of the Acoustical Society of America* 102 (5 Pt. 1) (Nov. 1997): 2780–2785.
39. See e.g., L. M. Brekhovskikh, O. A. Godin, *Acoustics of Layered Media I—Plane and Quasi-Plane Waves*, Ch. 4. (Springer, Berlin, 1990).

40. E.g. G. G. Sorrells, "A Preliminary Investigation into the Relationship between Long-Period Seismic Noise and Local Fluctuations in the Atmospheric Pressure Field." *Geophysical Journal* 26 (1–4) (Dec. 1971): 71–82; A. Ben-Menahem, S. J. Singh, *Seismic Waves and Sources*. (Springer, New York, 1981), Section 9.4.3.
41. For a theoretical treatment and experiments see F. Press, M. Ewing, "Ground Roll Coupling to Atmospheric Compressional Waves." *Geophysics* 16, (1951): 416–430; W. M. Ewing, W. S. Jardetzky, F. Press, *Elastic Waves in Layered Media*. (McGraw-Hill, New York 1957), Section 4.7.
42. This is shown directly in V. M. McCarthy, I. Dalins, "Frequency Shift in Air-Coupled Surface Waves Originated by Rocket Launches," *Journal of Geophysical Research* 76 (29) (Oct. 10, 1971): 7027–7034. See also I. O. Kitov et al., "An Analysis of Seismic and Acoustic Signals Measured From a Series of Atmospheric and Near-Surface Explosions." *Bulletin of the Seismological Society of America* 87 (6) (Dec. 1997): 1552–1562.
43. The theory of the two dilatational (compressional) wave types, a fast one where the fluid essentially moves with the solid and a slow one where the fluid essentially moves against it (plus a rotational (shear) type), was developed in M. A. Biot, "Theory of Propagation of Elastic Waves in a Fluid-Saturated Porous Solid. I. Low-Frequency Range." *Journal of the Acoustical Society of America* 28 (2) (March 1956): 168–178; M.A. Biot, "Theory of Propagation of Elastic Waves in a Fluid-Saturated Porous Solid. II. Higher Frequency Range." *Journal of the Acoustical Society of America* 28 (2) (March 1956): pp. 179–191. For measurements see e.g., C. J. Hickey, J. M. Sabatier, "Measurements of Two Types of Dilatational Waves in an Air-filled Unconsolidated Sand." *Journal of the Acoustical Society of America* 102 (1) (July 1997), 128–136.
44. H. E. Bass et al., "Coupling of Airborne Sound into the Earth: Frequency Dependence." *Journal of the Acoustical Society of America* 67 (5) (May 1980): 1502–1506; J. M. Sabatier et al., "Acoustically Induced Seismic Waves." *Journal of the Acoustical Society of America* 80 (2) (Aug. 1986): 646–649.
45. See e.g., H. K. Given, "Variations in Broadband Seismic Noise at IRIS/IDA Stations in the USSR with Implications for Event Detection." *Bulletin of the Seismological Society of America* 80 (6) (Dec. 1990): 2072–2088; J. A. Carter et al., "High-Frequency Seismic Noise as a Function of Depth." *Bulletin of the Seismological Society of America* 81 (4) (Aug. 1991): 1101–1114.
46. J. A. McDonald, T. G. Goforth, "Seismic Effects of Sonic Booms: Empirical Results." *Journal of Geophysical Research* 74 (10) (May 15, 1969): 2637–2647.
47. D. G. Albert, "Acoustic Waveform Inversion with Application to Seasonal Snow Covers." *Journal of the Acoustical Society of America* 109 (1) (Jan. 2001): 91–101.
48. D. G. Albert, J. A. Orcutt, "Acoustic Pulse Propagation above Grassland and Snow: Comparison of Theoretical and Experimental Waveforms." *Journal of the Acoustical Society of America* 87 (1) (Jan. 1990): 93–100; see also Albert 2001 (Note 47) and D. G. Albert, L.R. Hole, "Blast Noise Propagation above a Snow Cover." *Journal of the Acoustical Society of America* 109 (6) (June 2001): 2675–2681.
49. J. Altmann, S. Linev, A. Weiß, "Acoustic-Seismic Detection and Classification of Military Vehicles—Developing Tools for Disarmament and Peace-keeping." *Applied Acoustics* 63 (10) (Oct. 2002): 1085–1107; S. Linev, J. Altmann, A. Weiß, "Monitoring for Verification—Acoustic-Seismic Military-Vehicle Measurements of 2000 at Meppen, Germany." In: *Verification—Research Reports*, no. 11, Grünberg, Lenzen (2001).
50. P. Bormann, "Conversion and Comparability of Data Presentations on Seismic Background Noise." *Journal of Seismology* 2 (1) (1998): 37–45. The Values were Computed from the Power Spectral Density of Velocity at 10 Hz,  $4.1 \cdot 10^{-21}$  and  $1.8 \cdot 10^{-13}$

(m/s)<sup>2</sup>/Hz for low and high noise, respectively. Tables reproduced from J. Peterson, "Observation and Modeling of Seismic Background Noise." U. S. Geological Survey Open-File Report 93-322 (1993). Multiplying with 2 and a bandwidth of 100 Hz one gets mean square velocities of  $8.2 \cdot 10^{-19}$  and  $3.6 \cdot 10^{-11}$  (m/s)<sup>2</sup>, and the square root gives the rms values [see K. Aki, P. G. Richards, *Quantitative Seismology—Theory and Methods, vol. I*. Freeman: New York (1980), Section 10.2]. These are clear overestimates because the spectral power density decreases as the frequency increases above 10 Hz.

51. Altmann/Linev/Weiβ (Note 49), Linev/Altmann/Weiβ (Note 49).
52. M. M. Withers et al., "High-Frequency Analysis of Seismic Background Noise as a Function of Wind Speed and Shallow Depth." *Bulletin of the Seismological Society of America* 86 (5) (Oct. 1996): 1507–1515. Using their displacement power spectral density at 10 m/s mean wind speed at the surface of about 0.003 nm<sup>2</sup>/Hz (−25 dB re. nm<sup>2</sup>/Hz), multiplied with 2 and a bandwidth of 30 Hz results in a mean square displacement of 0.2 nm<sup>2</sup> and an rms value of 0.4 nm (see Aki/Richards (Note 50), Section 10.2). Multiplying the latter value with  $2\pi$  50 Hz (they measured up to 60 Hz), results in an rms velocity of 0.2 μm/s. At 6 m/s wind speed, the amplitude was about 1/6 of that. Wind-induced seismic amplitude decreased markedly with deeper geophones (to about 1/10 at −43 m), but in the present context one needs geophones very close to the surface. See also C. J. Young et al., "A Comparison of the High-Frequency (> 1 Hz) Surface and Subsurface Noise Environment at Three Sites in the United States." *Bulletin of the Seismological Society of America* 86 (5) (Oct. 1996): 1516–1528; Carter et al. (Note 45); Given (Note 45).
53. Altmann/Linev/Weiβ (Note 49), Linev/Altmann/Weiβ (Note 49). The wind speed during the 35-min period shown in Figure 6 resp. Fig. 6.10 of these references was evaluated for the present work.
54. Aki/Richards (Note 50), Section 10.2.
55. See e.g. Figure 14.17 in K. Aki, P. G. Richards, *Quantitative Seismology—Theory and Methods, vol. II*. (Freeman, New York, 1980).
56. Bhartendu, "A Study of Atmospheric Pressure Variations from Lightning Discharges." *Canadian Journal of Physics* 46 (4) (Feb. 15, 1968): 269–281; C. R. Holmes et al., "On the Power Spectrum and Mechanism of Thunder." *Journal of Geophysical Research* 76 (9) (March 20, 1971): 2106–2115; R. D. Hill, "Thunder." in R. H. Golde (ed.), *Lightning, vol. 1, Physics of Lightning*. (Academic, London, 1977); A. A. Few, Jr., "Acoustic Radiations from Lightning." In *CRC Handbook of Atmospherics, vol. II*. (CRC Press, Boca Raton FL, 1982).
57. Holmes et al. (Note 56).
58. This simplified model assumes independent superposition of all arrivals and neglects the longer path lengths of the later ones. See also Holmes et al. (Note 56).
59. Hill (Note 56), p. 395.
60. M. E. Kappus, F. L. Vernon, "Acoustic Signature of Thunder from Seismic Records." *Journal of Geophysical Research* 96 (D6) (June 20, 1991): 10,980–11,006.
61. E.g., Blumrich (note 1 of Figure 8); M. V. Lowson, J. B. Ollerhead, "A Theoretical Study of Helicopter Rotor Noise." *Journal of Sound and Vibration* 9 (2) (1969): 197–222.
62. E.g. J. C. Cook, T. Goforth, R. K. Cook, "Seismic and Underwater Responses to Sonic Boom." *Journal of the Acoustical Society of America* 51 (2 pt. 3) (1972): 729–741; J. E. Cates, B. Sturtevant, "Seismic Detection of Sonic Booms." *Journal of the Acoustical Society of America* 111 (1 pt. 2) (Jan. 2002): 614–628.
63. The apparent ground speed and N-wave duration vary with climb/dive angle, of course.

64. J. Altmann, "Acoustic and Seismic Signals of Heavy Military Vehicles for Cooperative Verification," *Journal of Sound and Vibration* 273 (4–5) (21 June 2004): 713–740; W. Kaiser, *Sound and Vibration from Heavy Military Vehicles—Investigations of Frequency Assignment and Wave Spreading with Respect to Monitoring under Disarmament Treaties*. Verification—Research Reports, no. 9, ISL, Hagen (1998).
65. Altmann (Note 64), Figure 8; Kaiser (Note 64), Section 3.2.2.
66. Of course, the line structure is more prominent in acoustic spectra, but can nevertheless be clearly seen also in seismic ones, see Kaiser (Note 64), Section 3.2.2; Altmann (note 64).
67. Blumrich (note 1 of Figure 8).
68. Altmann (Note 64).
69. See <http://www.globalsecurity.org/wmd/facility/images/gfafb.gif> (Oct. 1, 2004); the scale of the site diagram can be gained by comparing the city locations with a usual map of North Dakota.
70. At the end of 2004, there were deployed 500 Minuteman III and 10 Peacekeeper, the latter to be retired by Oct. 2005. R. S. Norris, H. M. Kristensen, "U. S. nuclear forces, 2005, NRDC Nuclear Notebook." *Bulletin of the Atomic Scientists* 61 (1) (Jan./Feb. 2005): 73–75.
71. In 2004, the silo-deployed ICBM numbers and types were: 120 SS-18, 130 SS-19, 15 SS-24 M1, 36 SS-27 (and there were 312 road-mobile SS-25). R. S. Norris and H. M. Kristensen, "Russian Nuclear Forces 2004, NRDC Nuclear Notebook." *Bulletin of the Atomic Scientists* 60 (4) (July/Aug. 2004): 72–74.
72. The extreme value has to be doubled since it can occur positively and negatively.  
 $\ln(4 \cdot 10^5) = \ln(4 \cdot 10^5)/\ln 2 = 18.6$ .
73. Plus maybe a slowly drifting DC offset of 1 or 2 bits.
74. For an example with horizontal propagation see Figure 4.11 in Kaiser (Note 64).
75. Here, the U. S. Sandia National Laboratories collaborated with the Russian Kurchatov Institute and the nuclear-weapons laboratory Arzamas-16, with main funding from the U.S. Department of Energy, to develop systems for remote monitoring of nuclear materials, Mosher et al. (Note 5), Chapter 4, option 2. See also "Russia: DOE MPC&A Program," [<http://www.nti.org/db/nis/profs/russia/forasst/doe/mpca.htm>] (Feb. 24, 2005).
76. [<http://www.kinemetrics.com>]; prices provided by E-mail in summer 2004.
77. A study should also look at the alternative method of infrasound detection at close range and compare the respective merits.
78. One such program has been developed under contract to the U.S. Air Force: M. J. White, Development of a Predictive Model for Rocket Launch Noise Footprint, Report for Air Force Research Laboratory, Littleton CO: Applied Research Associates, Nov. 27, 2000 (NTIS, AD-A384 661) (unfortunately, attempts to get access to this program were unsuccessful).
79. E.g., a program developed by the U.S. NASA: "Computer Program Predicts Rocket Noise," NASA Tech Briefs (Feb. 2001), [<http://www.nasatech.com/Briefs/Feb01/KSC12061.html>] (July 14, 2003) (however, access is limited to U.S. citizens and permanent residents).
80. Altmann (Note 64).
81. Mosher et al. (Note 5): Chapter 4, option 8.
82. Mosher et al. (Note 5): Chapter 4, option 4, approach 2.

83. Mosher et al. (Note 5): Chapter 4, option 8.
84. G. Forden, "Letter to the Honorable Tom Daschle on Further Options to Improve Russia's Access to Early-Warning Information", Washington DC: CBO, Sept. 3,1998, cited after Mosher et al. (Note 5), p. 46–47. These satellites on highly elliptical orbits would only function for three years.
85. [<http://www.ctbto.org>], Verification Regime, Overview (Feb. 24, 2005).
86. Annual Report 2003, CTBTO Preparatory Commission, Vienna (2004), Ch. 7, [<http://www.ctbto.org/reference/annualreport/ar-2003-mp7.pdf>] (Feb. 24, 2005).